



An Integrated BIM Planning Workflow for 3D Concrete Printing Projects

Jorge Rojas, S.M.ASCE¹; and Sogand Hasanzadeh, A.M.ASCE²

Abstract: Three-dimensional concrete printing (3DCP) is poised to address such critical challenges as low productivity in construction while offering design flexibility and material usage optimization. Although prior research focused on integrating digital design and fabrication to generate instructions for three-dimensional (3D) printers, existing approaches fall short of developing a building information modeling (BIM) model with the requisite detail for coordination with other construction activities and a lack of customization for defining the printing sequence. This paper streamlines the automation of the modeling process and generation of BIM parameters to consolidate project planning information within a unified level of development (LOD) 400 BIM model. The proposed workflow introduces an automation tool designed to enhance the LOD in 3DCP BIM elements from a lower LOD to LOD 400, which is suitable for fabrication. This proposed approach contributes to industry practices by providing an automated tailored solution for contractors to customize printing sequences and facilitate seamless coordination between 3D-printed elements and nonprinted components, improving overall project efficiency and precision. The outcomes shed light on project visualization and coordination through a detailed 3DCP BIM model and introduce planning parameters for enabling a printing strategy that can incorporate the contractor's expertise in contrast to other slicer software. DOI: 10.1061/JCCEE5.CPENG-6188. © 2025 American Society of Civil Engineers.

Author keywords: Building information modeling (BIM); Additive manufacturing; Three-dimensional concrete printing (3DCP); Visual programming.

Introduction

The construction industry lags behind other industries in terms of productivity due to challenges related to labor shortage and an aging skilled workforce (Kim et al. 2020). Additive manufacturing (AM) is gaining momentum because it eliminates the use of formwork, which leads to a reduction of labor usage (Siddika et al. 2020). Also, this technology increases productivity with a higher level of automation (Weng et al. 2021). Then, the elimination of labor-intensive activities like formwork and the automation of concrete placing reduce the need of labor, which seems like a promising solution to alleviate pressing problems related to the labor shortage in the construction industry (El-Sayegh et al. 2020). AM involves a digital fabrication technique wherein the material (e.g., plastics, concrete, or sand) is incrementally deposited layer by layer, following a predefined path dictated by a machine control code derived from a three-dimensional (3D) model.

In the realm of 3D concrete printing (3DCP), this process involves extruding a cement mixture, typically cement mortar, through a nozzle on a printing head. The utilization of 3DCP introduces numerous advantages, such as enhanced design flexibility for more intricate designs, that otherwise would be cost prohibitive with traditional formwork (Hossain et al. 2020). Also, 3DCP optimizes material consumption, reduces material waste, and

diminishes carbon dioxide emissions, all contributing to more sustainable construction practices (Alabbasi et al. 2023; Allouzi et al. 2020). Because 3DCP is an automated process that reduces the labor involved in manual tasks, it also helps boost productivity, enhance safety, minimize human errors, and increase precision, thus improving overall construction quality (Alabbasi et al. 2023; Allouzi et al. 2020; Botton et al. 2021). This emerging technology also potentially facilitates affordable housing construction, construction in remote regions, building shelters for populations affected by natural disasters, the provision of temporary military facilities, and the prospect of building extraterrestrial settlements (Allouzi et al. 2020; Davtalab et al. 2018; Tu et al. 2023).

However, regardless of all potential benefits of this technology there are also challenges related to a fragmented workflow that is not robust and is vulnerable to data loss, inefficient, and involves time-consuming file-transferring procedures between multiple software tools, increasing the probability of interoperability issues (Weng et al. 2021). Thus, this fragmented workflow does not align with building information modeling (BIM) because the BIM model is relegated to a simple 3D model instead of data repository of a built asset to facilitate decision-making during the project life cycle (NIBS 2020; Weng et al. 2021).

Although the prospect of placing BIM in tandem with 3DCP seems a logical pursuit, the workflow for 3DCP projects currently faces disruption due to a lack of integration between digital design and digital fabrication (Slepicka et al. 2021). The gap arises from BIM models not providing sufficient information for effective 3D printing process planning and 3D printing tools failing to use the critical information (e.g., printing speed, number of layers, and printing sequence) embedded within BIM models. A critical step toward achieving synergy and bridging this gap involves enhancing the level of detail that BIM models contribute to the planning phase of 3DCP projects. Moreover, it is imperative to adapt digital

¹Ph.D. Student, Lyles School of Civil and Construction Engineering, Purdue Univ., 550 Stadium Mall Dr., West Lafayette, IN 47907. Email: rojas27@purdue.edu

²Assistant Professor, Lyles School of Civil Engineering and Construction Engineering, Purdue Univ., 550 Stadium Mall Dr., West Lafayette, IN 47907 (corresponding author). Email: sogandm@purdue.edu

Note. This manuscript was submitted on May 19, 2024; approved on February 21, 2025; published online on May 29, 2025. Discussion period open until October 29, 2025; separate discussions must be submitted for individual papers. This paper is part of the *Journal of Computing in Civil Engineering*, © ASCE, ISSN 0887-3801.

fabrication workflows to fully capitalize on the wealth of information that BIM models bring to the forefront.

Accordingly, this paper builds a workflow that integrates the design and fabrication phases of a 3DCP project and enables the utilization of a BIM model with geometric and nongeometric data to establish a more efficient digital concrete fabrication. This paper sheds light on the integration of manual activities (e.g., plumbing) with the 3D printing process through the generation of a BIM model with sufficient detail of information for fabrication and assembly. This paper bridges the gap among digital design, digital fabrication, and assembly utilizing a single data repository—a BIM model—that consolidates all necessary information needed for design coordination, the generation of 3D printer instructions, and the integration and coordination of the printing process with other construction activities. The proposed integrated BIM workflow for planning facilitates enhanced visualization and coordination, enabling contractors to intervene with their expertise to define the printing strategy and sequence.

Background

Virtual environments (i.e., BIM, simulations, virtual reality, augmented reality, and mixed reality) and advanced manufacturing (i.e., AM, prefabrication, and modularization) are listed as the most promising areas for Construction 4.0 (Menegon and da Silva Filho 2022). This section delves into the latest advancements and practical implementations of both BIM and AM, providing insights into their current developmental status and specifically examining their collaborative utilization.

Additive Manufacturing in Architecture, Engineering, and Construction

Additive manufacturing offers a solution to the limitations of traditional manufacturing, also known as subtractive manufacturing (SM). Traditional manufacturing relies on such methods as molding or machining (drilling, chipping, milling, and grinding), which remove material from an initial volume to create a product's shape. These SM processes lead to higher costs due to specialized tooling or customized molds. Moreover, SM processes generate substantial waste from material removal (Manogharan et al. 2016). In contrast, AM produces less waste because it often requires only a single set of tooling and eliminates the need for using molds. Consequently, the emergence of 3D printing offers a compelling option and has already revolutionized various industries and applications [e.g., aerospace and aeronautics (Monteiro et al. 2022), automotive (Böckin and Tillman 2019), prototyping (Roscoe et al. 2023), electronics (Zikulnig et al. 2023), healthcare (Rezvani Ghomi et al. 2021), manufacturing (Hao and Lin 2020), education (Stern et al. 2019), military (Valtonen et al. 2023), architecture (Khamis et al. 2022), and more recently, construction (Delgado Camacho et al. 2018)].

The most popular application of AM in the construction industry is 3DCP. Depending on the specific 3D printer system, this process can be categorized into three main types: extrusion-based, binder jetting, or sprayed concrete techniques. Among the extrusion-based 3D printing techniques, notable examples include concrete printing, developed at Loughborough University (Buswell et al. 2018); contour crafting (CC) from the University of Southern California (Davtalab et al. 2022); and CONPrint3D from Technische Universität Dresden (Mechtcherine et al. 2019). The primary example of the binder jetting technique in 3D printing is D-Shape, created by Enrico Dini (Lowke et al. 2018), and the prominent technique for sprayed concrete is shotcrete-based

3D printing (SC3DP), proposed at Braunschweig University of Technology (Heidarneshad and Zhang 2022).

These 3D printing techniques have unique characteristics that make them more suitable for specific printing needs. For instance, SC3DP allows material deposition without being limited to a specific printing layer; this feature facilitates direct printing against preinstalled steel reinforcement. D-Shape excels at printing with high resolution, making it ideal for complicated shapes requiring a high level of detail. Conversely, CONPrint3D offers a coarser resolution but compensates with faster printing time due to the larger dimensions of the extruded filament. CC ensures a smoother surface finish compared with concrete printing or freeform printing, which involve extruding material freely without the use of trowels attached to the nozzle to smooth the surface (Lim et al. 2012). Out of the various 3DCP techniques, extrusion-based methods stand out as the most prevalent in the industry. Companies such as Winsun, ICON, COBOD, Apis Cor, XtreeE, and Cybe are actively adopting this approach in designing their 3D printers and 3DCP projects (Pessoa et al. 2021).

The preprocessing workflow for extrusion-based 3DCP resembles the procedure employed in fused deposition modeling (FDM), commonly used with desktop 3D printers. This workflow commences with the 3D modeling process. After the 3D modeling phase is finalized, preprocessing begins by creating a mesh representing the volumetric shape formed via interconnected triangular planes. This mesh is typically formatted as a stereolithography (STL) file, the most common format in the 3D printing industry (Sakin and Kiroglu 2017). Subsequently, specialized software, called a slicer, undertakes the slicing operation, which entails intersecting a plane parallel to the base of the 3D-printed object at the height of each printing layer. Often, this software allows for the specification of an infill pattern to establish material density within the printing contours. For each layer, a printing path is determined through optimization criteria, including prioritizing continuity, minimizing print time, or reducing idle intervals. The last step of the extrusion-based 3DCP preprocessing workflow involves generating a machine control code. This code constitutes a sequence of instructions sent to the 3D printer's computer. G-Code is the widely employed format for this control code, e.g., a computer numerical control (CNC) code (Smarsly et al. 2021).

Although the 3D modeling software possesses the capability to directly export models into a STL file or other 3D printing-compatible formats—such as wavefront object file (OBJ), additive manufacturing file (AMF), or 3D manufacturing format (3MF) (Kreider and Messner 2013)—contemporary BIM enables intelligent, data-rich models that incorporate information beyond mere geometry for better collaboration and analysis throughout the project life cycle. In the context of the BIM authoring tool, data workflow would be disrupted when using the STL file because the BIM model loses all nongeometric data. Simultaneously, data generated by the slicer software are not integrated into the BIM authoring tool. As a result, the BIM authoring tool would be relegated to the role of simple 3D modeling software and thereby fail to be used to its full potential. This issue introduces the gap in the workflow between digital design [computer-aided design (CAD)] and the subsequent digital fabrication stage, commonly known as computer-aided manufacturing (CAM) (Correa 2016).

Consequently, it is necessary to introduce a new workflow that seamlessly combines design and fabrication by creating a BIM model that retains enriched data and incorporates information generated during the slicing process. This BIM model should incorporate geometric and nongeometric data (attributes) that are generated from the slicing process spanning printing settings (layer height, width, and printing speed) and printing strategy (printing sequence,

phasing, and work zoning). Contractors can benefit from this AM preprocessing data for better planning and coordination of the printing process and other construction activities.

BIM Applications in 3DCP

BIM serves various functions, but two primary roles involve analyzing and communicating facility information stored within the digital model (Kreider and Messner 2013). The analysis function entails coordinating among project stakeholders to proactively identify issues before construction begins while ensuring the accuracy of the BIM model's information. On the communication front, BIM facilitates visualizing the model to assess whether the design intent is accurate and clear, and to consider whether the construction process planning is logical and feasible.

Challenges in BIM for 3DCP

A 3DCP project consist of three primary design development phases: establishing a comprehensive global geometry design for the building component, engineering the material distribution within this component (topology optimization), and detailing the fabrication process and toolpath layout needed for 3D printing the component (Bresghello and Naboni 2022). Multiple specialists need to manage each of the three phases, so this teaming constraint may result in a lack of seamless integration.

For instance, an architect often uses CAD software programs to design 3D-printed elements using standard boundary representation (BRep) modeling techniques. Using computer-aided engineering (CAE) tools, structural engineers will then define the cross section of the 3D-printed component, which includes reinforcement and material properties, given structural loads. Lastly, a 3D printing specialist or manufacturer will determine fabrication specifics, such as the number of layers, cross section of the 3D printing filament, 3D printer settings, toolpath layout, 3D printing sequence, and material attributes (e.g., buildability—resistance of fresh material to deformation under stress; pumpability—ability of material to be transported using a pump; and extrudability—ability of material to flow smoothly through the extruder) using CAM software. Additionally, professionals from various disciplines (e.g., electrical, plumbing, mechanical, roofing, and millwork) will then need to integrate their related design into a unified design complying with Design for Manufacturing and Assembly (DfMA) principles.

In conventional construction methods, assembly is conducted by skilled workers who rely on subjective interpretation of construction documents—e.g., drawings, specifications, detailing schemes, and project schedules—with a level of flexibility suitable for general guidance. In contrast, digital fabrication involves minimal human intervention, thus offering a limited margin for instruction flexibility. Thus, the precision of information is critical in digital fabrication because such information must be accurately communicated to computers for execution (Slepicka et al. 2021).

The concept of level of development (LOD) holds significance within the BIM methodology framework, denoting the extent of confidence that project team members can attribute to the information within the BIM model (BIMForum 2023b). For instance, LOD 100 corresponds to a conceptual representation of the model, whereas LOD 200 offers an approximate portrayal of its geometry, encompassing more detailed attributes such as quantities, shape, location, and orientation. LOD 300 signifies a precise geometry representation, facilitating direct measurements from the digital model. LOD 400 describes the model element with sufficient detail for fabrication, assembly, and installation, which means the model is developed to the level of shop drawings. LOD 500 culminates in an as-built model, reflecting the physical element's

actual construction and configuration. Fig. 1(a) shows the different LOD progression for a 3DCP element model specifying the design development phase, design specialist, and software application category.

Additionally, to these definitions for different LODs, BIM-Forum (2023a) also proposed the use of a Model Element Table in the Part I of the LOD specification, and the use of a Relevant Attributes Table in the Part II of the same specification. The Model Element Table describes each of the systems in a building using standard classifications systems (e.g., Unifomat, Omniclass, or Uniclass) and describes what should be included in the BIM model for a specific LOD. On the other hand, the Attribute Table describes each of the attributes that these previous elements should considered, describing the data type, units, and some examples of expected values. Because BIMForum LOD Specification does not have a specific definition for 3DCP Model Elements, the proposed Model Element Table is presented in Fig. 1(b). Similarly, because no attributes are defined for 3DCP model elements, a list of Relevant Attributes is proposed and documented in Fig. 1(c). Finally, Fig. 1(d) shows the geometry detail for the building systems of a 3DCP project.

Existing Solutions in 3DCP Workflows

Currently, BIM is widely used in traditional construction projects, but its use in 3DCP projects is still being investigated. There have been several attempts to combine BIM with 3DCP (e.g., Abadia et al. 2020; Abadia and Smarsly 2021; Smarsly et al. 2021). For instance, researchers have explored an approach called printing information modeling (PIM), which uses an Industry Foundation Class (IFC) scheme. In one study, this approach was applied to a single-story five-wall building to incorporate concrete printing details (such as contour lines and filament paths) into the model; this information was then used for slicing and generating a toolpath (Abadia et al. 2020). Similarly, a parametric BIM model of a hexagonal column was developed to assist in the manufacturing process, specifically for the slicing and planning toolpaths (Abadia and Smarsly 2021).

Another PIM study created an IFC-based BIM model to gather geometry and materials information from it (Smarsly et al. 2021), where an L-shaped wall was sliced into only two layers, and toolpaths were generated for each layer; these toolpaths were then used to create a CNC code for a gantry 3D printer. One of the most important advantages of this latter method was that the IFC file provided data on material properties that could then be used to adjust the printing speed and pump pressure of the 3D printer based on the concrete material's extrudability and buildability.

A more sophisticated approach is the Planning and Operations Control Software for Automated Construction (POCSAC), which is a customized interoperable BIM-integrated system that enables the interaction, analysis, and control of the components of a robotic 3D printer (Davalab et al. 2018). POCSAC is also based on the IFC schema, resolving interoperability issues with a BIM authoring tool and enabling the data extraction required for material preparation and robot control from an IFC file exported from a BIM model. The BIM model geometry analysis defines and translates an optimized toolpath into commands for a robotic 3D printer (G-Code). Data extracted from models related to material properties are then used for material designing and laboratory testing. Then, a construction report of the 3D printing process is generated and stored for future projects.

Another method involves utilizing Dynamo, a visual programming tool that functions as a plugin for Revit, which is a widely used BIM authoring tool in the architecture, engineering, and construction (AEC) sector. In this approach, the goal is to derive curves

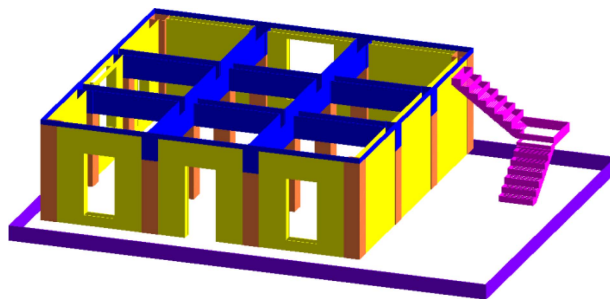
LOD	LOD 100	LOD 200	LOD 300	LOD 400	LOD 500
DESIGN PHASE	CONCEPTUAL DESIGN	APPROXIMATE GEOMETRY	PRECISE GEOMETRY	FABRICATION ASSEMBLY	AS-BUILT
DIGITAL MODEL					
DESIGN DEVELOPMENT	GLOBAL GEOMETRY DESIGN		TOPOLOGY OPTIMIZATION	TOOLPATH LAYOUT	CONSTRUCTION
SPECIALIST	ARCHITECT		ENGINEER	MANUFACTURER	CONTRACTOR
DESIGN TOOL	CAD / BIM		CAE /BIM	CAM /BIM	BIM

(a)

System	Classification*	Inclusions	Attribute Table	Color
Standard Foundations	A1010 21-01 10 10 Ss 20 05	3D printed formwork	3DCP	
Structural Column	B1010.10.12 21-02 10 10 10 12 Ss 20 30 75 15	3D printed formwork	3DCP	
Floor Decks, Slabs, and Toppings	B1010.20.40 21-02 10 10 20 40 Ss 30 12 85 18	3D printed formwork	3DCP	
Structural Stairs	B1080.20 21-02 10 80 10 Ss 35 10	3D printed formwork	3DCP	
Exterior Wall Construction	B2010.20 21-02 20 10 20 EF 25 10	3D printed shell, infill, formwork	3DCP	

*Uniformat / Omniclass / Uniclass

(b)



(d)

Attribute	Data Type	Units	Option Examples
Layer Width	Number	mm	25 mm
Layer Height	Number	mm	10 mm
Layer Order	Text	-	"L001", "L002", "L003", etc.
Printed Element	Text	-	"Foundation", "Column", "Wall", "Slab", etc.
Printed Component	Text	-	Shell, Infill, Formwork
Printing Speed	Number	-	250 mm/sec
Printing Workset	Text	-	"WS001", "WS002", etc.
Printing Work Zone	Text	-	"WZ001", "WZ002", "WZ003", etc.
Printing Sequence	Text	-	"WS001-L001-WZ001", etc.
Layer Length	Number	m	10 m
Printing Time	Number	min	60 min
Cross Area	Number	m ²	250 mm ²
Printed Volume	Number	m ³	1 m ³
Printing Cost	Number	USDS	USDS 1000

(c)

Fig. 1. Level of development for 3DCP building system: (a) LOD progression sample for schematic design of 3DCP wall; (b) proposed model element table, Part I: element geometry based on BIMForum; (c) proposed relevant attribute table, Part II: associated attribute information for LOD 400–3DCP Building System based on BIMForum; and (d) geometry representation of 3DCP building system.

resulting from the intersection of a BIM element with a plane parallel to its base. These curves serve as the contour for a toolpath. By generating a point cloud with specified intervals along these curves, the necessary points for guiding the extruder head are obtained. These points can then be used as instructions for robotic programming plugins, such as KukulPrc, to simulate the movements of the robotic arm during the 3D printing process (Forcael et al. 2021). A similar strategy utilized Dynamo for Revit to create a geometry model of 3D-printed walls, specifically the 3D printing filaments for the outer layer of the wall and the interior infill geometry. The geometry also excluded window openings and doorways from the 3D-printed structure (He et al. 2021). However, a limitation of this approach is the lack of consideration of 3D printing layers.

Consequently, although the modeling phase was completed, such subsequent stages as slicing, toolpath planning, robot kinematics simulation, and machine control code generation could not be addressed.

To address this limitation, it becomes necessary to use a traditional workflow (such as slicers, robotic simulators, and robot programming tools), but this constraint leads to a fragmented data flow after the modeling phase. A comparable method utilizing Dynamo for Revit was employed by some researchers to filter concrete walls from a BIM model, subsequently slicing them. This process led to the extraction of the perimeter contours and infill curves, which served as blueprints for organizing the toolpath layout for each 3D printing layer. After gathering all points from various layers

Table 1. Application areas of BIM for 3DCP identified by comprehensive review of previously published studies

Research area and reference	Application areas					
	A ₁	A ₂	A ₃	A ₄	A ₅	A ₆
PIM-IFC slicer for walls (Abadia et al. 2020)	—	X	—	X	—	—
IFC-slicer for column (Abadia and Smarsly 2021)	—	X	—	X	—	—
PIM-IFC slicer for L-wall (Smarsly et al. 2021)	—	X	—	X	—	X
POCSAC (Davtalab et al. 2018)	—	X	—	X	—	X
KukalPre slicer for column (Forcael et al. 2021)	—	X	—	X	X	X
Dynamo modeling for walls (He et al. 2021)	—	—	X	—	—	—
Dynamo slicer for walls (Weng et al. 2021)	X	X	X	X	—	X
BIM collaborative simulation (Teng et al. 2023)	X	X	X	X	X	X
BIM deep learning (Du et al. 2024)	X	X	X	X	X	X

and toolpath layout curves (perimeter and infill), these points were rearranged to establish a continuous printing path. With the points systematically arranged, a machine control code could then be produced using the G-Code format. This code guided the 3D printer to follow a predetermined sequence of actions (Weng et al. 2021).

A recently published study used Dynamo to generate the toolpath for a 3D-printed wall with a ring-shaped footprint. In this study, Teng et al. (2023) adjusted the toolpath to incorporate vertical reinforcement within the wall without interfering with the infill pattern. Then, using a separate robot programming software, they integrated two separate programs to control two robotic arms working in collaboration to simulate the printing process and rebar installation (Teng et al. 2023). In other research, Du et al. (2024) utilized Dynamo to generate the printing path for the robotic arm and extract the coordinates of the rebar location. In this physical experiment, a single robotic arm was programmed for printing and installing reinforcement in a small rectangular 3D-printed component using a depth camera and a deep learning model; however, because the same robot was performing both tasks, the printing process was interrupted to swap the extruder for a gripper.

Each of these past attempts reveals why it is essential to investigate new ways to enhance BIM models with fabrication-relevant data for streamlined analysis and coordination across various disciplines during the design, fabrication, and construction phases. Furthermore, the current state of the art reveals the need for establishing an improved workflow that goes beyond adapting desktop 3D printing tools and instead develops specialized CAM tools tailored for construction-oriented 3D printing applications.

Points of Departure

A comprehensive list of the gaps in knowledge and the applications derived from previous studies is discussed in the following. Seven gaps in knowledge have been identified in the literature related to BIM for 3DCP construction:

- G₁: Focused on a single building component (walls), not a building system.
- G₂: Neglected openings for doors and windows within the models.
- G₃: Lacked such construction details as steel support and 3D-printed formwork.
- G₄: Assumed simplified continuous 3D printing path—lacked stop-start commands.
- G₅: Focused on the simulation of robot kinematics, not the construction process.
- G₆: Not considered a LOD suitable for fabrication modeling.
- G₇: Generated the machine control code primarily for simple geometry.

Table 1 summarizes previous application areas explored in the literature related to BIM for 3DCP. A total of six BIM application areas were identified in the literature for the 3DCP preprocessing workflow:

- A₁: Filtering concrete elements from a BIM model.
- A₂: Slicing concrete elements into 3D printing layers.
- A₃: Generating an infill pattern inside perimeters of 3D-printed elements.
- A₄: Generating toolpath plan.
- A₅: Simulating robotic 3D printer kinematics.
- A₆: Generating machine control code.

Given these gaps of knowledge and past applications, two problems are affecting the interfacing of BIM with 3DCP:

1. Previous efforts have only implemented a BIM model for 3DCP at LOD 200 instead of the LOD 400 necessary for fabrication. The problem with a 3DCP BIM model at a LOD lower than 400 is that 3DCP is not an isolated automated process and therefore requires coordination with various manual tasks during the 3D printing process. Consequently, a fragmented workflow—i.e., one in which the BIM model does not include all the information related to the fabrication process—will not optimally harness the full potential of BIM to offer analysis (coordination), communication (visualization), and efficient planning of the construction process.
2. Current construction printing software does not account for the fundamental characteristics of 3DCP construction. Instead, they replicate manufacturing slicers initially designed for FDM desktop 3D printers and lack customization for 3DCP applications. Such a limitation signifies that the 3DCP workflow conforms to pre-existing tools rather than adapting to the unique nature of 3DCP projects. Thus, developing an AEC-adapted slicer software is necessary to accelerate the adoption of 3DCP in construction (Mechtcherine et al. 2019).

These two identified problems motivated the two objectives of this paper. Firstly, this paper develops a 3DCP BIM model LOD 400 that incorporates the digital fabrication process offered by 3DCP with sufficient resolution to incorporate BIM's granular construction visualization and coordination features. The proposed LOD 400 contains the requisite data needed for the 3D printing process (i.e., 3D printing sequence) while also feeding data from the 3D printing process back into the BIM model (e.g., printing layer height, filament width, infill path, and number of layers). The model can also coordinate the 3D-printed design alongside other traditional construction processes (e.g., manual installation of steel support, formwork, and rough-ins) and can integrate the workflows of other construction tasks (e.g., mechanical, plumbing, and electrical). Consequently, the built model integrates the necessary functions to plan a 3DCP fabrication process effectively.

Secondly, this paper proposes and validates a new framework to streamline the preprocessing workflow of 3D concrete printing and to incorporate enough detail of the fabrication phase into the BIM model for the planning process. The proposed details for a 3DCP model enable AEC users to customize the printing sequence and strategy, addressing limitations associated with existing CAM tools (i.e., slicer software). Thus, the proposed framework and model will demonstrate the coordination and visualization of 3D printing details while also integrating traditional BIM capabilities for planning a 3DCP project.

Specifically, this research aims to address the seven critical knowledge gaps by proposing and validating an automated BIM framework for designing and constructing a complete 3D-printed building system (G_1 and G_7), incorporating detailed considerations for various wall openings such as doors and windows (G_2). It will also address the construction details of 3D-printed formwork for cast-in-place elements, including columns and foundations (G_3). In addition, the proposed framework will introduce noncontinuous printing paths that involve strategically interrupting the extrusion process to accommodate the unique requirements of large-scale on-site 3DCP (G_4). The proposed framework will further include the precise geometric definitions of each printed layer, facilitating the coordination of the 3D printing process with the manual installation of non-printed components (G_5). Moreover, the proposed framework achieves LOD 400, providing a high level of detail suitable for fabrication, including the geometric and nongeometric attributes of all printed components and specific printing settings for accurate execution (G_6).

Workflow Development and Proposed Method

To automate generating a BIM model and information parameters (LOD 400) for all components of a 3DCP project (e.g., shell, infill, formwork filaments, and steel supports), the research team devised and executed a set of Dynamo scripts for Revit. This model furnishes the comprehensive information necessary for the fabrication phase of a 3DCP project with the possibility of enabling users to customize the printing strategy.

Fig. 2(a) provides a general overview of the research scope. The problem statement highlights the current fragmented workflow identified in the literature, where it is typically extracted from a BIM model at LOD 200 to generate the G-Code for 3D printer commands, and critical slicing process information is not integrated into the BIM model. To address these limitations, this paper proposes a comprehensive workflow that incorporates an integrated BIM data repository at LOD 400 with sufficient granularity for planning a 3DCP project.

The proposed workflow has been validated by utilizing it for planning, coordination, visualization, and executing a customized printing strategy. For the planning validation, the 3D-printed layers of the model are organized by phases and work zones. In terms of coordination and visualization, the enriched model facilitates clash detection between printed layers and other building components. Regarding the optimized printing strategy, this can be converted into G-Code for seamless 3DCP execution.

Fig. 2(b) outlines the proposed workflow, which encompasses automating the modeling of 3D-printed layers (e.g., shell and infill formwork), and enriching the model with BIM parameters essential for planning. These planning parameters are embedded into the model as attributes that store information related to the phasing, work zoning, printing sequence, and printing speed. The resulting LOD 400 is validated for BIM uses including visualization and coordination and utilized for machine control, which involves

generating customized code for the 3D printer. This printing code extracts the waypoints (x - y - z values) from the model and the printing settings, such as printing speed and sequencing. The workflow was tested and validated through rapid prototyping using a 3D printer.

BIM Modeling Using Dynamo for 3DCP

The initial step in modeling all 3DCP components involves the creation of materials to represent each component type. Within this context, Dynamo facilitates the predefinition of the essential input data necessary for generating material types within Revit. These input data encompass various parameters, including specifying the alpha, red, green, blue (ARGB) color assigned to represent the material within Revit, determining the rendered appearance, and assigning a distinct material name for subsequent use in material schedules to support quantification purposes. For instance, within a 3DCP project, the materials catalog may range from a fundamental configuration—such as defining a single 3DCP material for all extruded filaments in the project—to a more complex setup involving the specification of distinct 3DCP materials for each unique element type (e.g., walls, columns, foundation, horizontals, and stairs).

Fig. 3 shows the results of the Dynamo script developed for this purpose: Fig. 3(a) illustrates the initial representation of a cast-in-place (CIP) concrete model, wherein each element type is distinguished by a unique material color. The representation of Fig. 3(b) narrows its focus to solely the 3D-printed filaments, employing a unified material type denoted as 3DCP. Finally, Fig. 3(c) demonstrates distinct material types assigned to each element, exemplifying the potential complexity of material differentiation in this context.

In a 3DCP project, four main components are involved: the shell or perimeter filaments, the infill filaments, the formwork filaments, and the steel mesh support. Fig. 4 displays images of actual 3DCP projects where these components have been identified.

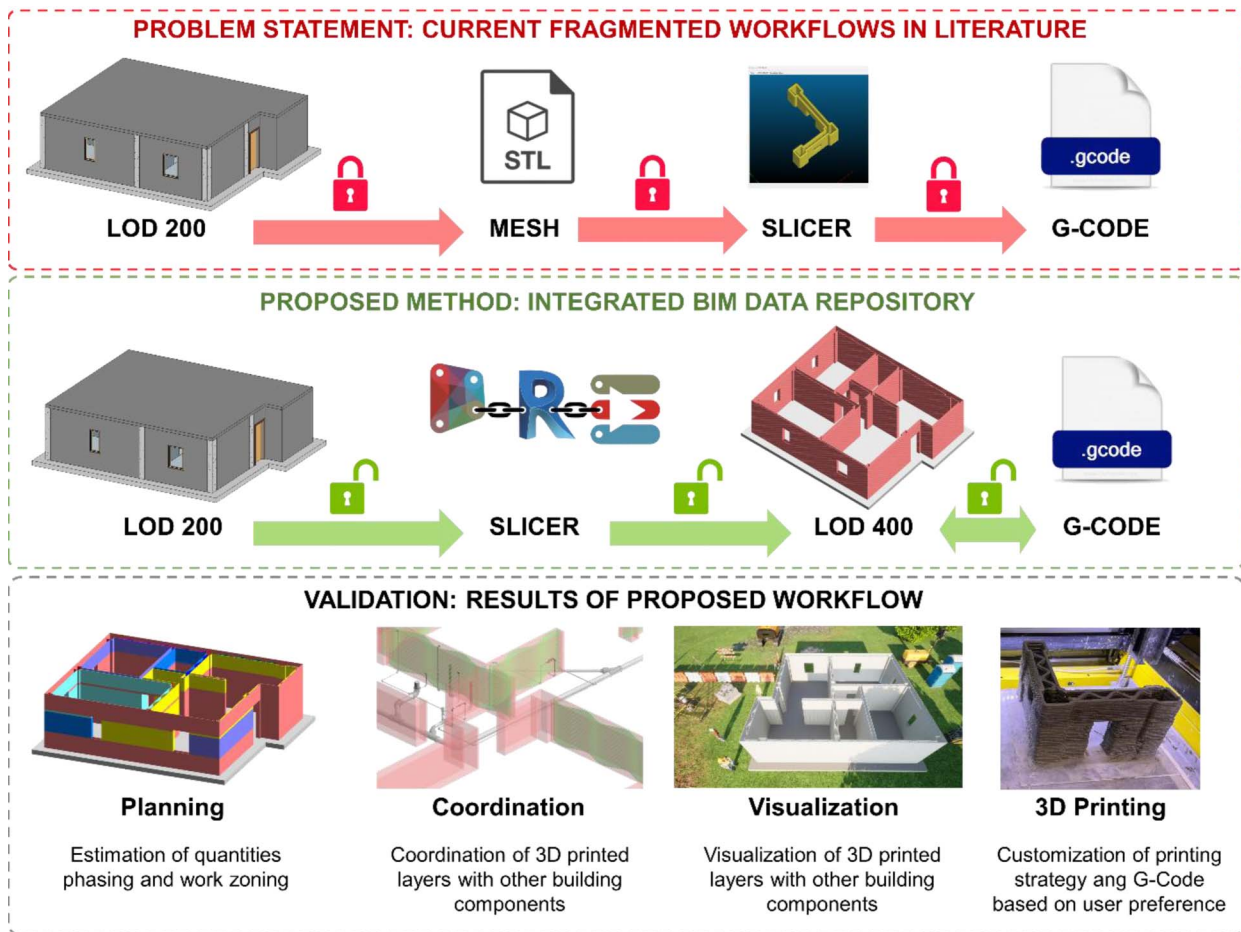
The shell filaments are 3D-printed layers that are visible on the interior or exterior of the building; these shells primarily shape hollow walls and other vertical elements. Figs. 4(a–c) show examples of the shell for 3DCP hollow walls.

The infill filaments or infill patterns serve a dual purpose: they provide stability during the 3D printing process and enhance the structural integrity once the mortar hardens (Bos et al. 2022). Fig. 4(d) exhibits a common infill sinusoidal wave pattern used for 3DCP.

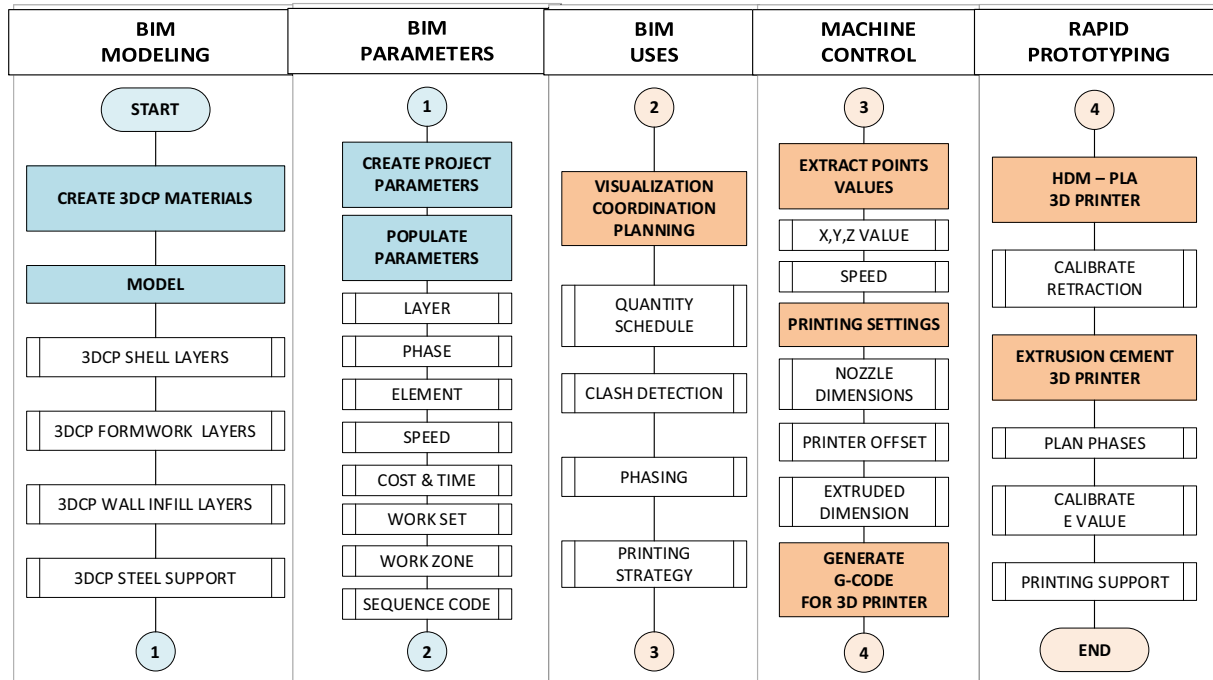
The formwork filaments consist of 3D-printed mortar layers that act as stay-in-place (SIP) formwork. These filaments are used to cast lightweight concrete within the cavity after steel reinforcement has been installed, creating a conventional reinforced concrete (RC) column integrated into the hollow walls, as displayed in Figs. 4(b and c) (Buswell et al. 2018).

An alternative to supporting the infill mortar involves using steel mesh ladders, similar to the construction of cinder block walls. This alternative printing support embedded within the printed structure can be seen in Figs. 4(a–c) (Guamán-Rivera et al. 2022).

The primary component of a 3DCP element is the shell, which defines the shape of a hollow element. This shell is created by extruding material along a predefined path corresponding to the desired hollow shape's contour. When dealing with a single element, such as a wall or column, this path is determined by the perimeter of that individual geometry. However, when multiple elements—for instance, a wall with a column—are joined together, only the outer perimeter of the combined elements is considered as a single hollow shape. To clarify these concepts, Fig. 5



(a)



(b)

Fig. 2. Proposed method for implementing a LOD 400 BIM model for a 3DCP project: (a) research overview: problem, method, and validation; and (b) proposed workflow overview.

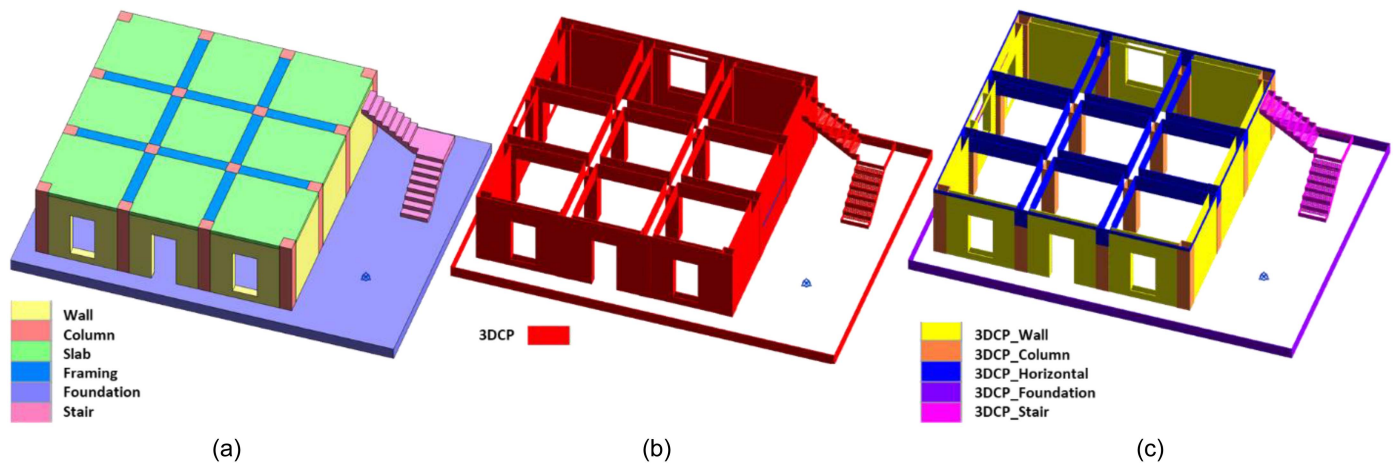


Fig. 3. Model of 3DCP: (a) CIP elements; (b) 3DCP filaments; and (c) 3DCP filaments for each element type.

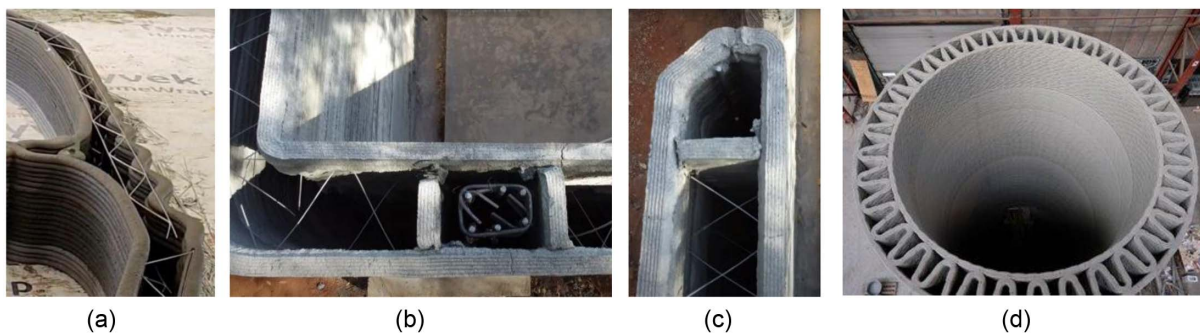


Fig. 4. (a–c) Steel mesh ladders for 3D printing support (credit: Black Buffalo 3D); (b and c) SIP-3D-printed formwork for columns (images courtesy of Jarett Gross, with permission); and (d) infill pattern (credit: Cobod International).

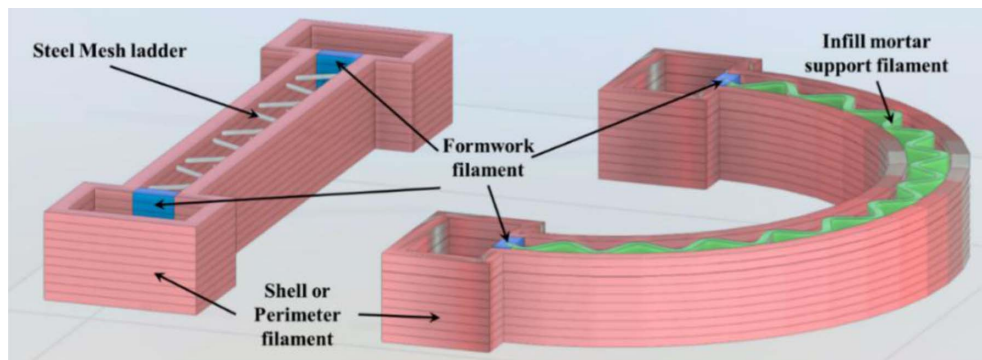


Fig. 5. 3DCP components (i.e., shell, infill, and formwork filaments, and steel support).

distinguishes the modeled components generated with the proposed Dynamo scripts. Here, the shell filaments of columns and walls when they are combined, the shutter or formwork filaments used to cast concrete columns, the infill mortar support filaments, and the steel mesh support embedded within the printed form are all indicated.

Some modeled designs may choose an alternative approach that would involve treating the shell of each column separately and then completing only the two faces of the hollow wall that connect to the

two columns. Although such a printing approach is also valid, opting for a single shell for combined elements offers the advantage of extruding a continuous path without interruptions. This choice is particularly beneficial for enhancing the aesthetics of the exposed layers. Starting and stopping the extrusion operation on the deposited filaments can lead to such issues as material overfill, which can lead to deformations and affect the overall aesthetics (Buswell et al. 2018). If start/stop operations cannot be avoided, then planning them on the nonvisible layers is recommended. Such considerations

embedded within the model can streamline and facilitate the fabrication process and underscore the benefit of including the 3DCP process within a BIM model.

The modeling process of the 3DCP components (i.e., shell, formwork, infill, steel) was automated with a toolset consisting of four scripts (one for each component) using Dynamo 2.13.

Dynamo Script for Shell Filaments

The workflow consists of four steps, as depicted in Fig. 6(a). The first step generates the model mesh surface. Initially, elements are selected from the BIM model, from which their respective geometries are extracted. In this context, the solid representation of these elements is then combined into a single unified solid through a Boolean union operation. Subsequently, a mesh surface is derived for this composite solid using the Dynamo node Mesh.ByGeometry. Second, a bounding box containing the solid union created by the selected elements is formed. Additionally, offset planes are defined at each extrusion layer height and oriented respectively to the bottom face of the bounding box.

Third, the workflow slices the structure and generates two-dimensional (2D) contour paths. Within this phase, each of the previously established planes intersects with the mesh to generate 2D contour curves, which ultimately define the toolpath.

The fourth and final step encompasses the actual modeling of the 3DCP shell filaments, utilizing the Solid.BySweep node and employing the cross section of the printed filament as the profile to be extruded along the path defined by the 2D contours. To complete this process, an element of the Generic Model type is created by utilizing the extruded solid as the geometry source to generate the corresponding Revit element within the 3DCP model.

Dynamo Script for Formwork Filaments

To automate the modeling process for the 3D-printed formwork filaments, as illustrated in Fig. 6(b), the process begins with a BIM model of the concrete structure. Then, the procedure entails the selection of faces designated for casting the concrete columns (user-driven or predefined for all columns in model) and slicing the selected faces to identify the curves that represent the extrusion path. The next step is to determine the toolpath, which involves trimming the selected face width to the desired toolpath length to avoid overlapping filaments. The extrusion of the filament will then start, utilizing the Dynamo node Solid.BySweep. This operation uses the filament section as a profile and employs the trimmed curve as the path. Finally, the outcome manifests as a Generic Model, seamlessly integrated into the BIM model. The extruded

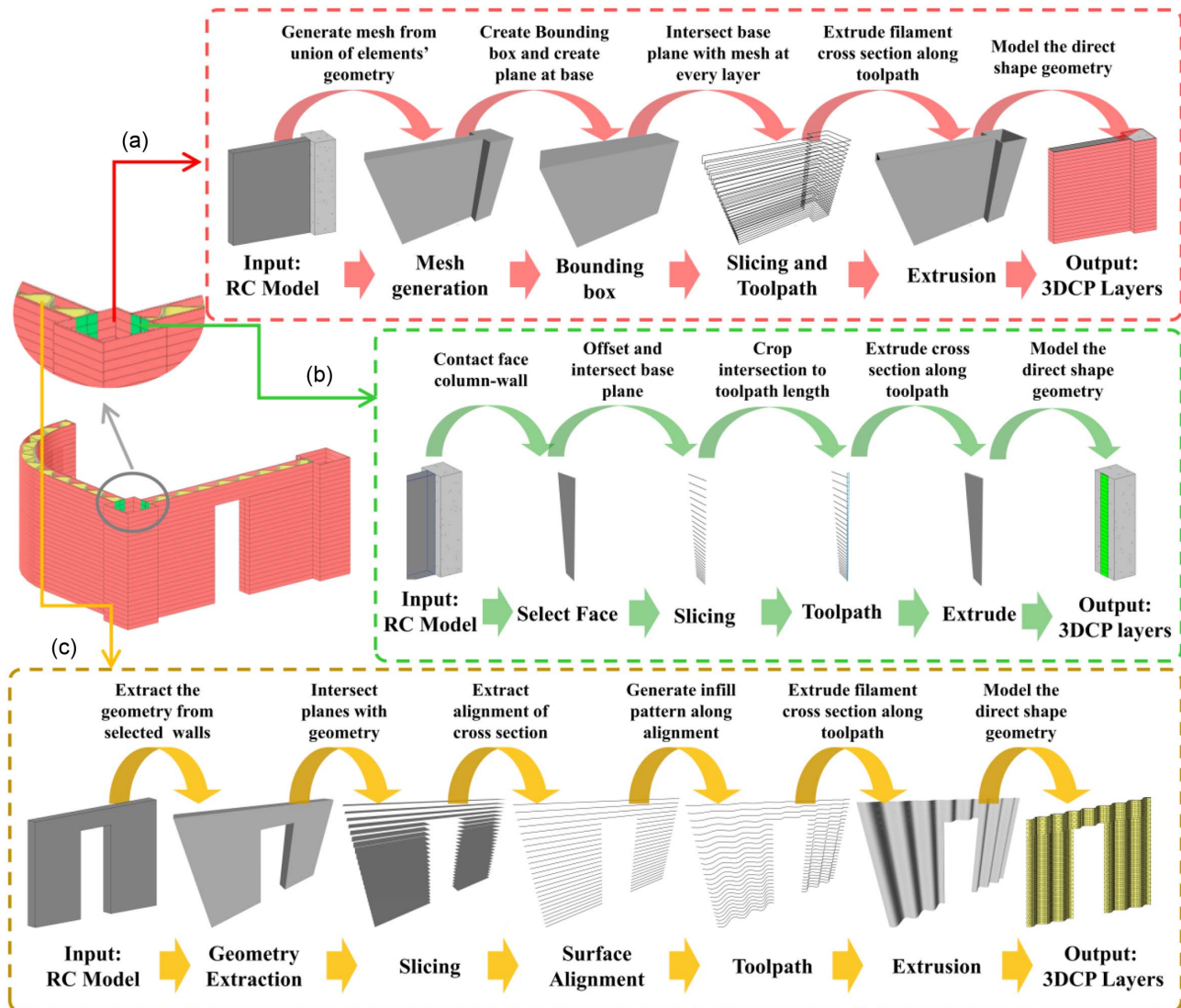


Fig. 6. Workflow for modeling automation: (a) 3DCP shell filaments; (b) 3DCP formwork filaments; and (c) 3DCP infill filaments.

geometry serves as the source for this new addition, as highlighted in green in Fig. 6(b).

Dynamo Script for Infill Filaments

Fig. 6(c) visually outlines the modeling process of the 3D-printed infill filament. In this instance, the cross section of the selected element geometry is acquired through the slicing process. Subsequently, the alignment of each sliced region is utilized as a guide for generating the toolpath. In this case, in particular, the toolpath curve is defined by a zigzag shape or follows a sinusoidal function to avoid sharp corners that, due to robot inertia, may reduce printing speed, as suggested by Bos et al. (2022). Utilizing element cross-section alignment generated during the slicing process offers a scalable solution.

Whether dealing with straight or curved walls, the resulting sinusoidal function seamlessly adheres to the wall's alignment, as illustrated in Fig. 7. Another notable advantage of the proposed cross-section alignment lies in its intelligent capacity to exclude openings for windows or doorways when generating the infill pattern.

Dynamo Script for Steel Support

The workflow closely resembles the infill workflow but with two key distinctions. First, the slicing process is not generated for every layer; instead, it is selectively employed for every s number of layers spacing in between steel support. Secondly, the extruded section is based on the circular cross section of the steel support rebar, as opposed to the rectangular cross section of a 3D-printed filament (layer height and width). The simplified flowchart for the four scripts in Dynamo is shown in Fig. 8. The corresponding flowchart for the shell script is highlighted in Fig. 8(a), the flowchart for the formwork is in Fig. 8(b), and the corresponding ones for the infill and steel support are in Fig. 8(c).

The aforementioned four modeling steps provide a fabrication model for the 3DCP components, including the shell, formwork bulkhead, infill, and steel support. However, these elements are mainly only geometry—with some minor materiality—and lack other parameters related to the printing process. Therefore, the next step should focus on enriching the model with nongeometric data—such as the printing sequence, speed, time, and cost—to capture the benefits of BIM.

Populating BIM Parameters Using Dynamo

The defined 3DCP components share common parameters essential for the 3D printing process. Fig. 9 provides a summary of all implemented Dynamo scripts with the respective number indicating the

recommended order in which each script should be executed to enrich the 3DCP model with all the parameter values. The developed toolbox of individual Dynamo scripts enables the users to adjust only the required parameters.

The first Dynamo script is Create Parameters, and it creates all the empty project parameters within the Revit BIM model. Each parameter is defined by a parameter name (e.g., 3DCP_WorkSet, 3DCP_Layer, 3DCP_Element, and so on), group (e.g., construction), data type (e.g., length, area, volume, text, or numeric), and model category (e.g., Generic Model). The second script is named Layer, and it computes the values of the 3DCP_Layer parameter. For this task, the Dynamo script creates a bounding box for each filament, then determines the minimum and maximum elevation of the box and computes the layer number by comparing one layer's height with the elevations of the bounding box.

The third script is named Element, and it computes the values for the 3DCP_Element parameter by intersecting each filament with each category (i.e., structural wall, structural column, foundation, stairs, and so on) and assigning the corresponding element type to the filament. This parameter value was utilized to generate color-coded models like the one used in Fig. 3(c). The fourth script is named Component, and it is used to define the 3DCP_Component parameter. For this script, the workflow only needs to retrieve the Generic Model element name (i.e., shell, infill, formwork, and steel) and assign the corresponding string value in the parameter. The name of the Generic Model element was assigned when using each of the Dynamo scripts for automated modeling of the 3DCP components.

The fifth Dynamo script is Speed, and it defines the parameter 3DCP_speed for each of the filaments in the model. Typically, the printing speed is constant during the whole printing process due to the slicer software limitations of the printing settings. However, with the proposed approach, the user can define specific speeds for each filament. High speed in the top layers may increase the load in the bottom layers, creating deformations because cement mortar needs time to gain enough strength for buildability (Buswell et al. 2018; Hoffmann et al. 2020). Then, a faster printing speed can be considered for the bottom layers and a slower speed for the top layers (Smarsly et al. 2021). The proposed script allows the user to define a specific speed for various layers. Therefore, the proposed script enables the user to print faster at the bottom and slowly at the top layers, which would not be possible with traditional slicers.

The sixth script is named Planning, and it computes several planning parameters (i.e., 3DCP_Volume, 3DCP_Area, 3DCP_Length,

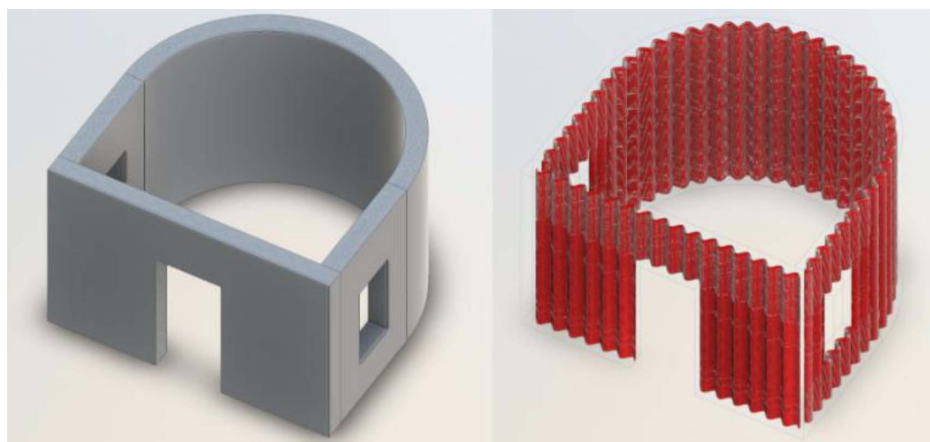


Fig. 7. Scalable automated model infill pattern generated by the customized Dynamo script.

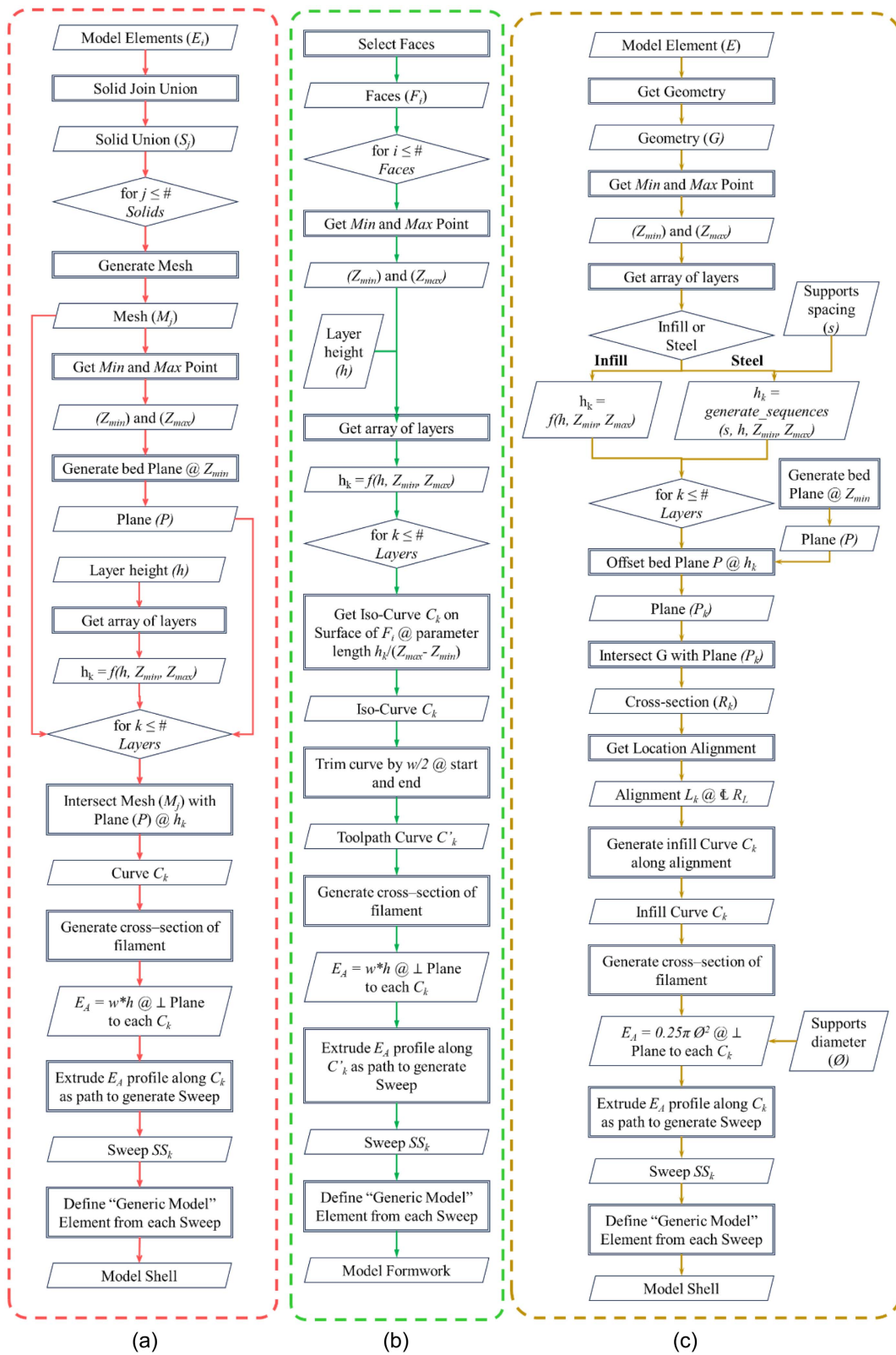


Fig. 8. Simplified flowchart for automated modeling of 3DCP components: (a) workflow for modeling layers on shell; (b) workflow for modeling layers as formwork; and (c) workflow for modeling infill layers.

3DCP_Time, and 3DCP_Cost). The volume and area values are extracted directly from the solid geometry. The length can be estimated by dividing the volume by the cross-section area of the filament (width \times height). The time (min) for each of the filaments

can be estimated from the ratio of the filament length (mm) and the printing speed (mm/min), and the cost could be an estimation based on the unit cost (USD/m³) multiplied by the filament volume (m³).

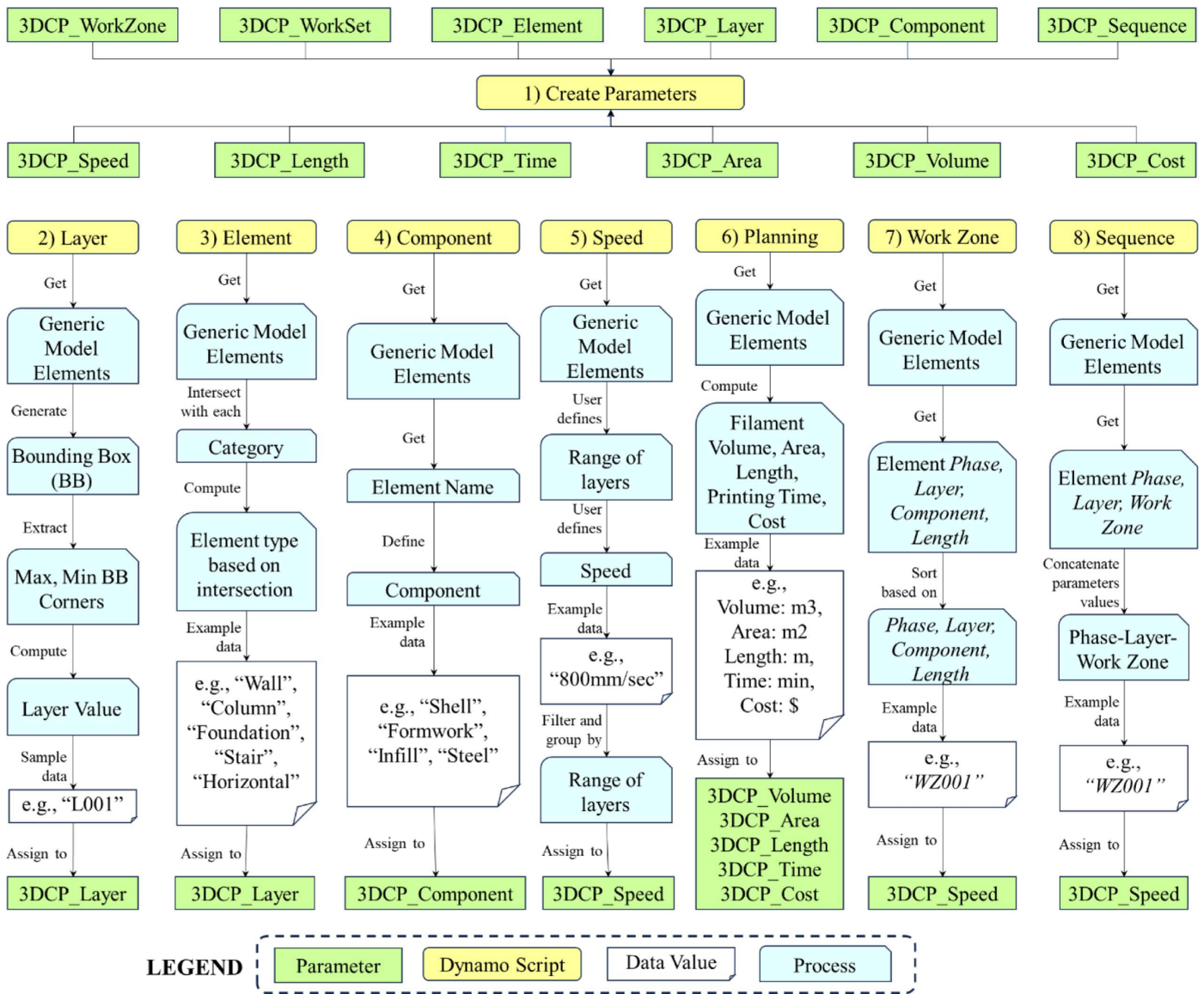


Fig. 9. Simplified Dynamo scripts workflow to create and populate 3DCP parameters.

A key feature of the proposed BIM planning approach is enabling the user (contractor) to customize the printing strategy. Typically, the contractor plans the construction strategy by defining the work sets (construction phases) (WS) and work zones (workspaces) (WZ) using workload leveling techniques like takt planning, where a parade of trades will follow a construction sequence (Jabbari et al. 2020). In the context of a 3DCP project, a work set groups a subset of layers of a specific portion of the building (construction phase), and the work zones will represent each of the individual filaments that are in a specific layer of each work set. Then, the work set will define the order in which the whole 3DCP project will be built by phases (group of layers), and the work zone will define the order in which the filaments are deposited in a specific layer within each work set. Fig. 10(a) shows a model for all the work sets of the 3DCP model, and Figs. 10(b and c) show the work zoning for Work sets WS001 and WS002, respectively.

In this case, the 3DCP_WorkSet parameter is defined manually by the user by selecting a group of layers in the model. However, a specific Dynamo script named Work Zone was implemented to populate the 3DCP_WorkZone parameter. This script will sort the filaments, starting with the shell filaments, then the infill,

and finally, the formwork. For this research, the criteria are based on leaving the not visible filaments to the end to avoid any aesthetic problems due to stopping and starting the material extrusion (Buswell et al. 2018) and having a boundary filament to content the infill and formwork. In the case of multiple filaments of the same component type, priority is given to the largest filament.

The last script of the proposed Dynamo toolbox is named Sequence, and it computes the 3DCP_Sequence parameter values. This parameter is a string that results from concatenating the work set value (e.g., WS001), the layer (e.g., L001), and the work zone (e.g., WZ001) resulting in the formation of a unique sequence code (e.g., WS001-L001-WZ001). Fig. 10(d) shows a fully implemented 3DCP model enriched with all the 3DCP parameters after running all the scripts proposed with the Dynamo toolbox.

Rapid Prototyping Using a Polylactic Acid FDM Desktop Printer and a Cement-Based 3D Printer

A Dynamo script was developed by the research team to generate a G-Code compatible with LulzBot TAZ 6 (Lulzbot, Fargo, North Dakota). The proposed tool received the 3DCP BIM model as

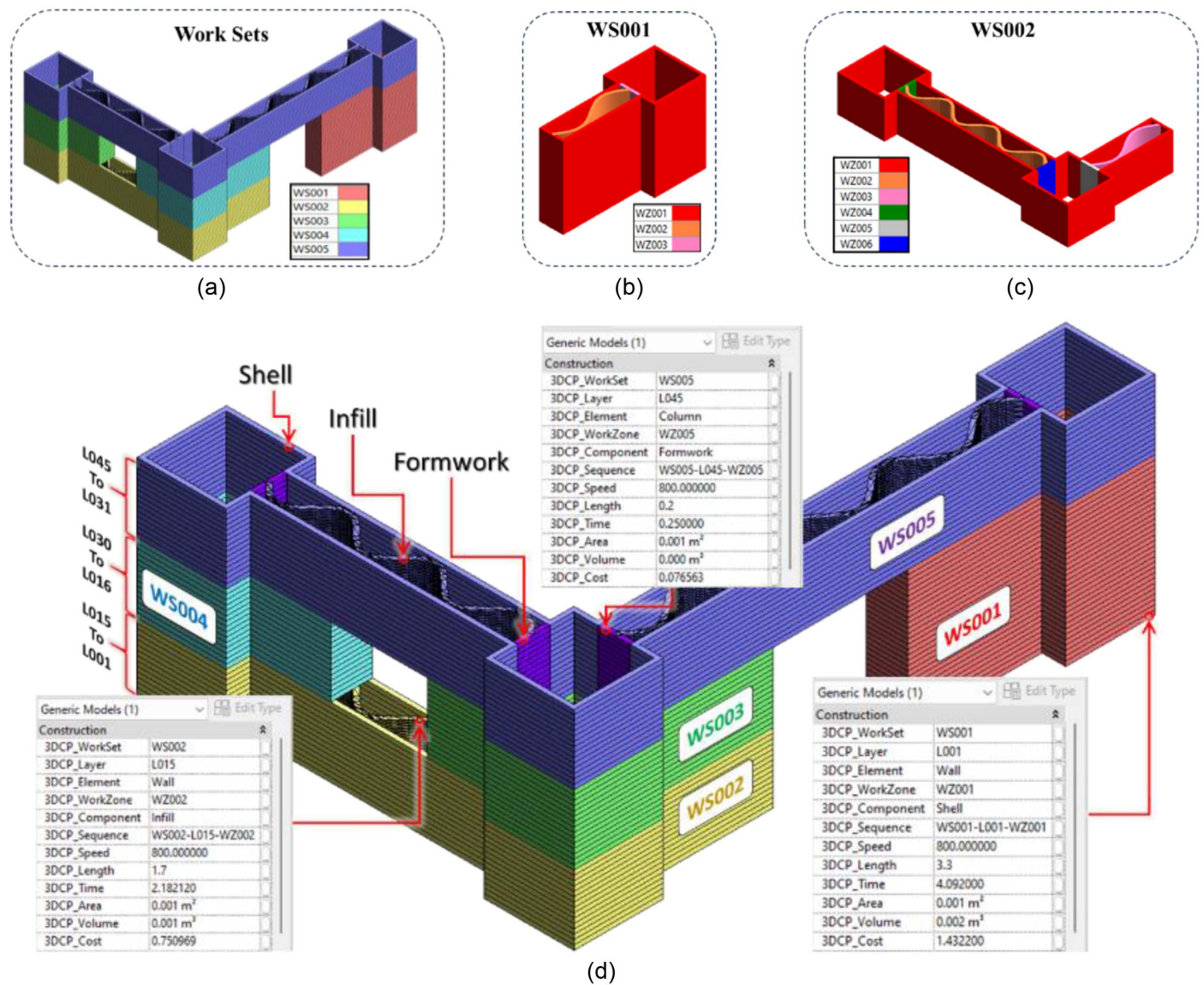


Fig. 10. Representations of a 3DCP model for planning (phasing and work zoning): (a) work sets; (b) work zones in WS001; (c) work zones in WS002; and (d) 3DCP model enriched with parameters for planning.

input, which was enriched with the planning parameters and the printer settings defined by the user. In this case, due to the reduced scale of the 3D-printed sample and the size of the printhead [Fig. 11(a)], the model can only be printed by completing all filaments in a layer before moving to the next one [Fig. 11(b)] without any option to move below the last printed layer.

The proposed Dynamo script starts by selecting all the 3DCP elements in the model, then filters and groups all elements into shells, infills, and formwork in separate lists. For the list of shell filaments, the script intersects the geometry mesh with a plane crossing at the mid-height of the filament mesh and extracts the outer contour, Polycurve. Then, the centerline (toolpath) for the shell filament is obtained by offsetting the previous Polycurve by half the width of the printed filament to its interior. Then, the Polycurve is split into individual curves and the start and end points of each curve are extracted to obtain the x -, y -, and z -coordinates. The last step consists of creating a list that stores the information for each point (work set, layer, work zone, x , y , z , and speed).

A similar process is conducted for the formwork filaments, but in this case, the script extracts the surface resulting from

intersecting the filament mesh with a mid-height plane. Then, the script uses the node `Surface.GetIsoline` to extract the centerline (toolpath) of the formwork filament. Similarly, to the shell filaments list, all the points data (work set, layer, work zone, x , y , z , and speed) is stored in a formwork list. In the case of the infill filaments, the script first extracts all the vertices of the filament mesh and then a Python script node computes the centerline (toolpath). The Python script pairs the points of both the inner and outer sides of the mesh filament and then gets the equidistant points for each pair. The centerline of the infill filament (toolpath) is the curve resulting from joining all middle points. Similar to the shell and formwork, a third list of points data is stored in an infill list.

The next step is to arrange all the previous lists (i.e., shells, infills, and formwork) into a matrix G [Eq. (1)]. This matrix will serve as an input to a Python script node responsible for writing the G-Code compatible with the LulzBot printer. This G -matrix stores all the points data information (i.e., work set, layer, work zone, x , y , z , and printing speed) as shown in Eq. (1)

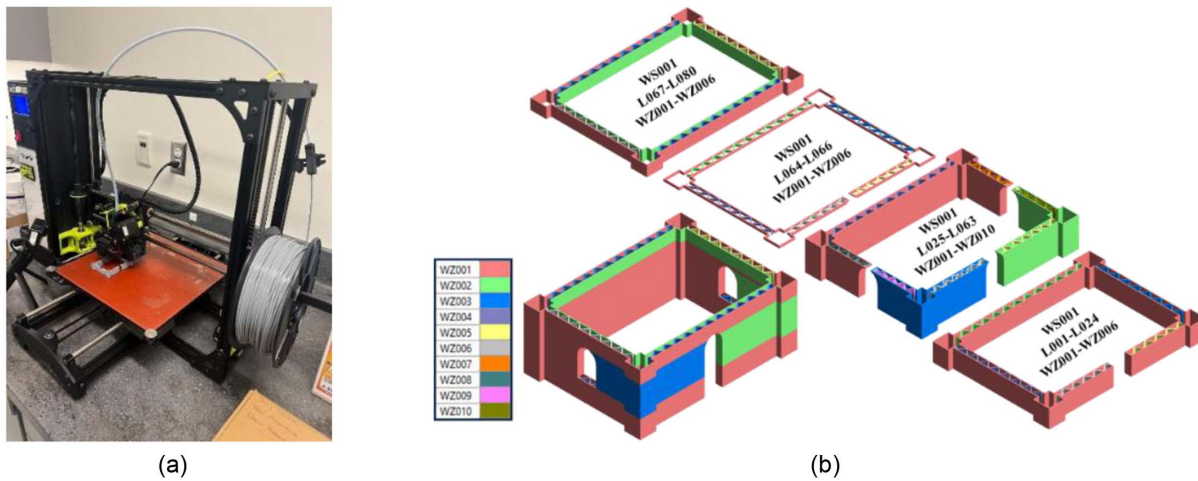


Fig. 11. BIM 3DCP planning: (a) Lulzbot printing BIM model; and (b) phasing and work zoning.

$$G = \begin{bmatrix} WS_1 \\ \vdots \\ WS_n \end{bmatrix} \begin{bmatrix} L_1 \\ \vdots \\ L_n \end{bmatrix} \begin{bmatrix} WZ_1 \\ \vdots \\ WZ_n \end{bmatrix} \begin{bmatrix} x_1 \\ \vdots \\ x_n \end{bmatrix} \begin{bmatrix} y_1 \\ \vdots \\ y_n \end{bmatrix} \begin{bmatrix} z_1 \\ \vdots \\ z_n \end{bmatrix} \begin{bmatrix} S_1 \\ \vdots \\ S_n \end{bmatrix} \quad (1)$$

The final step of the Dynamo script consists of the Python script node (G-Code generator) that provides the printer instructions in a G-Code file. The inputs for this node are the scale factor, the start printing position of the prototype in the printer bed, the *G*-matrix, and the minimum values for the point coordinates (*x*, *y*, and *z*) from the entire toolpath.

The scale factor is the ratio between the filament layer heights of the prototype [height (*h*) of polylactic acid (PLA) filament

manufactured by Polymaker (Houston, Texas) polyacid] and the BIM model (*H* large-scale filament height). The start point input defines the location of the prototype in the Lulzbot coordinate reference system (CRS), whose origin is in the upper right corner of the printing bed. The *G*-Matrix stores all the information related to every point in the toolpath, and the minimum values for *x*, *y*, and *z* are used to relocate the BIM model to the origin of the CRS in Revit. Fig. 12 shows a summary of the entire proposed Dynamo script workflow. This flow chart summarizes the Dynamo script, highlighting the user inputs needed and the Python script nodes, which were described in detail previously.

Similar to the previous Dynamo script, a customized version was implemented to generate a G-Code compatible with a cement-based 3D printer (Hydra 16A, Hyrel, Norcross, Georgia). The script

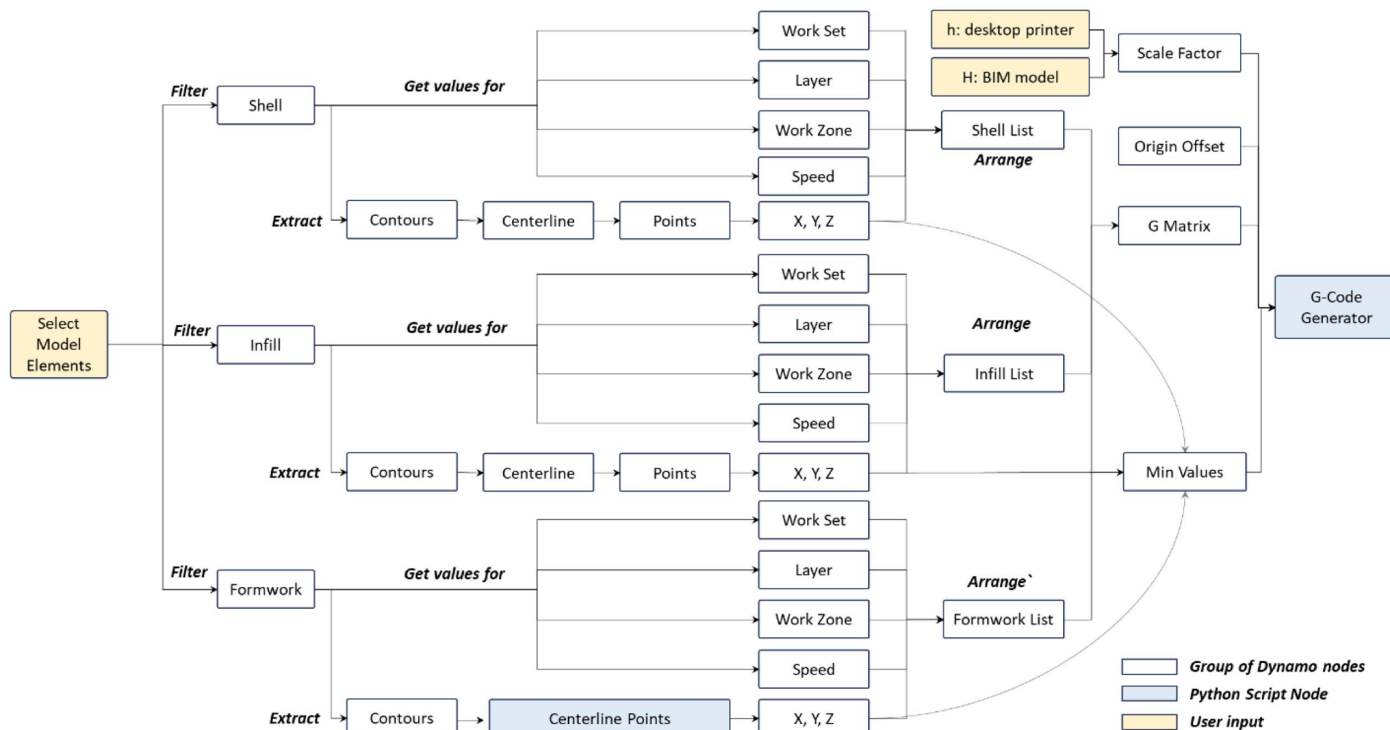


Fig. 12. Simplified representation of Dynamo script for G-code generation.

only needs slight changes, mainly in the Python node responsible for writing the G-Code compatible with the Hyrel printer. In this case, instead of a skirt just does a very short run outside of the prototype footprint to minimize the material waste. Then, for the traveling mode, instead of using the command G0, this script writes the G1 but considers a minimum extrusion value (E0.1). This command combination keeps priming the extruder at the same time that is not extruding a new filament in the traveling path.

Validation of the 3DCP BIM Model

To validate the efficacy of using the proposed workflow for 3DCP planning, the research team tested the toolbox to generate different 3DCP BIM models with sufficient granularity of information for the planning and fabrication process. Then four criteria (three qualitative and one quantitative) are used to validate the workflow. For the qualitative criteria the proposed framework enables user to (V_1) extract quantities for planning material demand, (V_2) coordinate and visualize the 3DCP components with other nonprinted components (i.e., steel support and plumbing), and (V_3) customize the printing strategy by defining printing phases. On the other hand, for the quantitative criterion, the proposed framework enables users to (V_4) tailor the printing sequence as key performance indicator (KPI) to reduce the printing time compared with a traditional slicer as a baseline.

Estimation of Quantities for Planning a 3DCP Project (N_1)

The proposed toolbox was tested to generate the enriched BIM model of a 2 bedroom and 1 bathroom (2B1B) apartment. Then, the information was extracted automatically in a quantity schedule using Revit 2023. Fig. 13 shows the results of the Dynamo workflow using a 3D view of the BIM model and the schedule of quantities that allow users to better understand and plan the amount of material required for each layer and phase (i.e., WS001–WS004). This is particularly important when phases (work sets) need to be considered to level the work on different workdays. The schedule

stores geometric data (volume) and nongeometric data (i.e., cost, and time), which are particularly important for construction managers. The 3DCP parameters allow easy grouping and filtering based on the layer, the work set (phase), and component types (shell, formwork, and infill).

Coordination and Visualization of 3D-Printed Components with Nonprinted Components (N_2)

The same 2B1B apartment model was used for the coordination and visualization of the 3D-printed components (i.e., shell, formwork, and infill filaments) versus other non-printed components (i.e., steel support and plumbing). Traditional slicers only focus on the toolpath representation as linework but lack integration with other nonprinted components (i.e., steel support and pipelines). In addition, BIM models with low granularity of detail do not represent the printed filaments on the model. With the proposed approach, a higher detail resolution of the fabrication components (filaments) can be automatically generated and included in the clash detection analysis with other nonprinted components.

The BIM model resulting from the proposed toolbox is an input for the clash detection process of a 3DCP project. Figs. 14(a and b) show the result of using the 2B1B model for the visualization of the 3DCP project. The BIM model was used to define the layout for the plumbing pipelines because the filament geometries are included in the LOD 400 BIM model. The pipes can be adjusted to avoid clashes between the infill (filaments) and the pipes. Fig. 14(c) demonstrates the clash detection process using Navisworks Manage version 2023 and the 3DCP model generated with the Dynamo toolbox.

Rapid Prototyping Using 3DCP BIM Model (N_3)

To validate the efficacy of the Dynamo tool developed for this research, three printing tests were conducted. The first test used the desktop printer LulzBot TAZ 6 with PLA material. The second and third printing tests utilized the Hydra16A printer from Hyrel and mortar cement material. The second test consisted of printing a

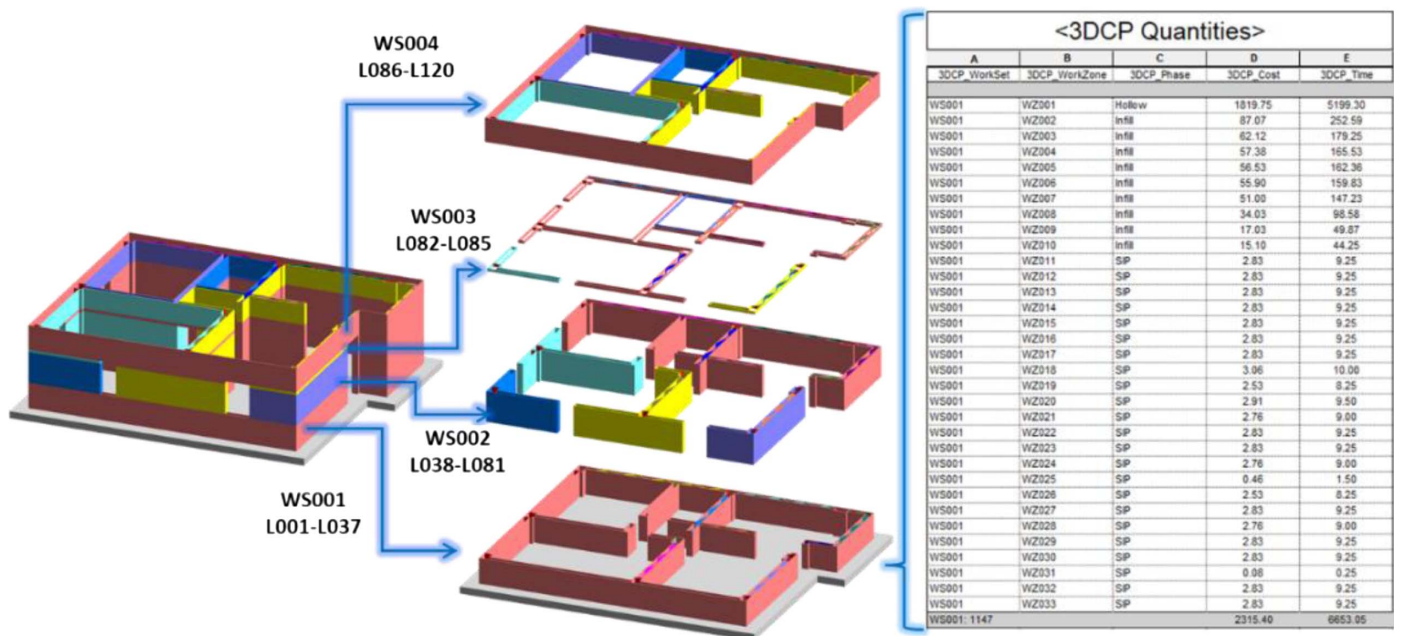


Fig. 13. BIM model with WS and WZ, which in turn yield quantities schedules for planning.

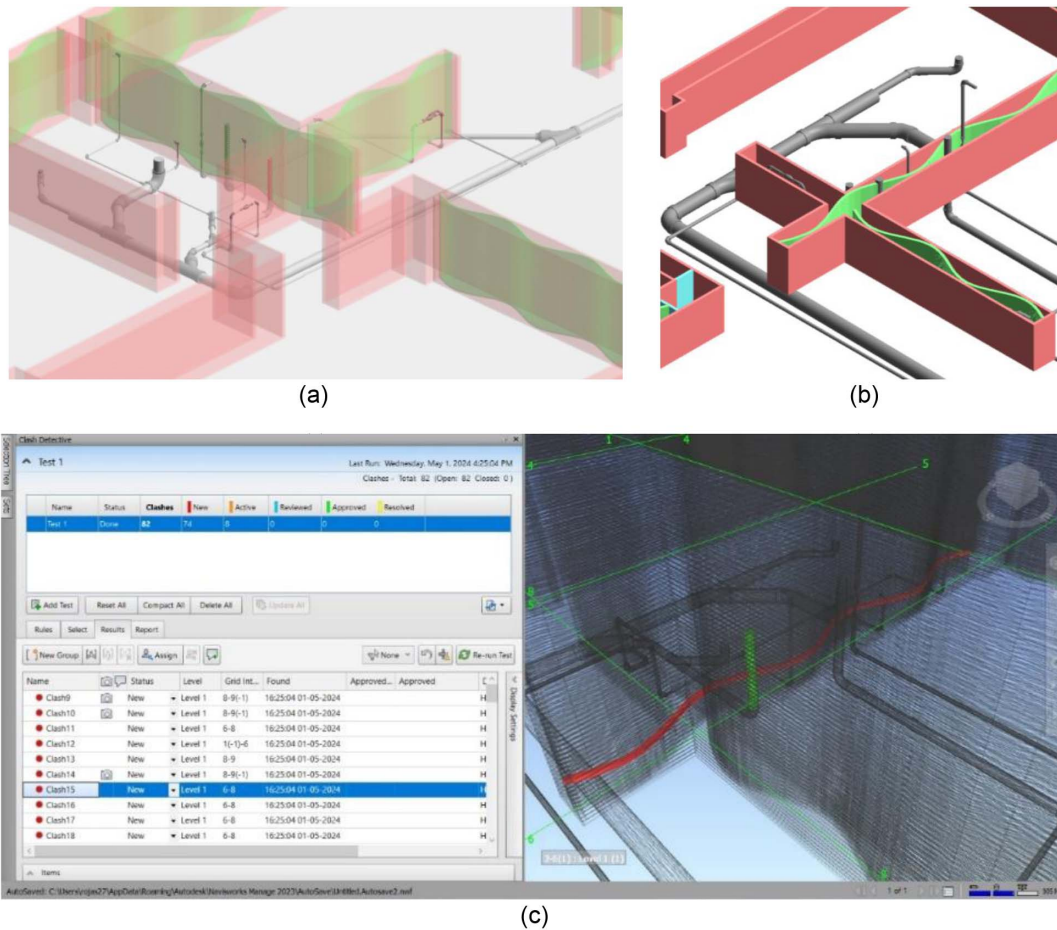


Fig. 14. Coordination and visualization of 3DCP BIM model: (a and b) 3D view of 3DCP model and plumbing; and (c) clash detection in Navisworks Manage.

sample using a small shoring system for the doorway and window openings (onsite 3DCP). The third test involved printing the sample in three phases (work sets) for posterior assembly (off-site 3DCP).

Rapid Prototyping with LulzBot TAZ 6

Three samples were printed using the Dynamo slicer developed by the researchers. Fig. 15(a) shows the three different results by



Fig. 15. Printing samples and quality evolution to adjust printing settings.

changing the printing settings in the Dynamo slicer: printing speed, traveling speed, and retraction value. For comparison, three more samples were printed using the Cura LulzBot slicer with different infill densities. The results with the Cura slicer are shown in Fig. 15(b).

Rapid Prototyping with Hyrel Hydra 16A for Onsite 3DCP

A test was conducted using the proposed Dynamo slicer to generate a G-Code compatible with a Hyrel Hydra 16A printer. This Hyrel printer can extrude cement mortar, which better resembles the conditions of a 3DCP project than a PLA printer. Fig. 16(a) shows the test results that include the use of a 3D-printed PLA formwork to support the overhead layers above the windows and door openings. The results show that the G-Code generated with the Dynamo slicer works properly and all data can be extracted automatically from the BIM model.

Rapid Prototyping with Hyrel Hydra 16A for Offsite 3DCP

Fig. 16(b) shows a 3D-printed model test that was printed in three phases (work sets). This experiment explored the idea of printing the pieces for posterior assembly to avoid a shoring system emulating an offsite construction process. Accordingly, the three work sets (WS001, WS002, and WS003) were printed directly onto the printer bed, rather than being printed on top of each other. This approach expedited the printing process and optimized printer utilization because all layers were successfully printed in a single day, without the constraints typically associated with the buildability of fresh mortar and eliminating the need for formwork.

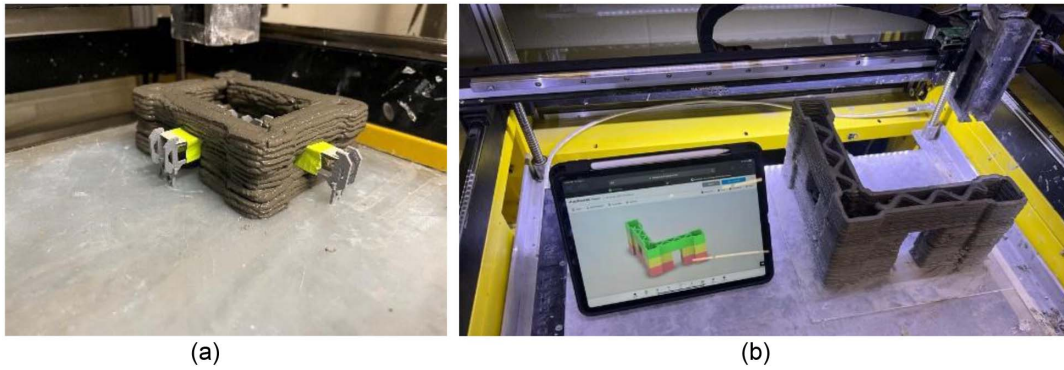


Fig. 16. Prototype 3D print using G-Code generated using Dynamo script for a Hyrel Printer: (a) onsite 3DCP with Hyrel; and (b) off-site 3DCP with Hyrel.

Analysis of the Printing Strategy (N_4)

Construction work activities can be classified into three primary categories: productive work (PW), contributory work (CW), and noncontributory work (NCW) (Brioso and Calderon-Hernandez 2023). Productive work directly contributes value to production and propels progress (e.g., bricklaying, formwork erection, and so on), whereas contributory work is essential but does not enhance progress or add value to the activity (e.g., mortar mixing, stripping formwork, and so on). In contrast, noncontributory work is neither essential to the task nor does it augment its value (e.g., waiting for instructions or materials).

In the context of a 3DCP project, the time associated with PW encompasses the printer extruding material and depositing layers. Then, the productive time (T_{PW}) can be estimated by the ratio of each filament length (l_{ijk}) and the printing speed (Sp_{ijk}). In the case of the work associated with CW relates to the printer traveling without printing. Then, the contributory time (T_{CW}) can be estimated as the ratio of the traveled distance (D_{ijk}) and the traveling speed (St_{ijk}). Finally, the NCW relates to all the time the printer has idle time due to interruptions or unnecessary traveling movements. Then, the noncontributory time (T_{NCW}) can be estimated as the sum of all the times the printer is not moving (interruptions) or making unnecessary movements. Eq. (2) presents all three components

$$T = T_{PW} + T_{CW} + T_{NCW} = \sum_{i=1}^{WS} \sum_{j=1}^L \sum_{k=1}^{WZ} \frac{l_{ijk}}{Sp_{ijk}} + \sum_{i=1}^{WS} \sum_{j=1}^L \sum_{k=1}^{WZ} \frac{D_{ijk}}{St_{ijk}} + \sum_{i=1}^n T_i \quad (2)$$

To evaluate the performance improvement due to the possibility of incorporating the user strategy into the printing process, a baseline was established using a G-Code generated by Simplify3D, a commercial slicer for desktop printers (Cincinnati, Ohio). Then, two samples (i.e., an L-shaped model with a window opening and a doorway) were printed using the baseline and the proposed Dynamo slicers. Both G-Codes were tested using the Hyrel printer. Because the test for running the G-Codes needs to be executed without interruptions to minimize NCW time, the volume of one sample must be less than the syringe capacity (150 cm³). For this experiment, the estimated volume required for the L-shaped sample was 118.4 cm³ and due to the scale and printing resolution, no infill was considered.

Fig. 17 shows the estimated printing times using the baseline and Dynamo slicers. The printing settings for both slicers were defined as the same: the layer height was 3 mm, the filament width was 6 mm, 15 layers in total, the printing speed was 750 mm/min, the traveling speed was 1,000 mm/min, and the infill density was

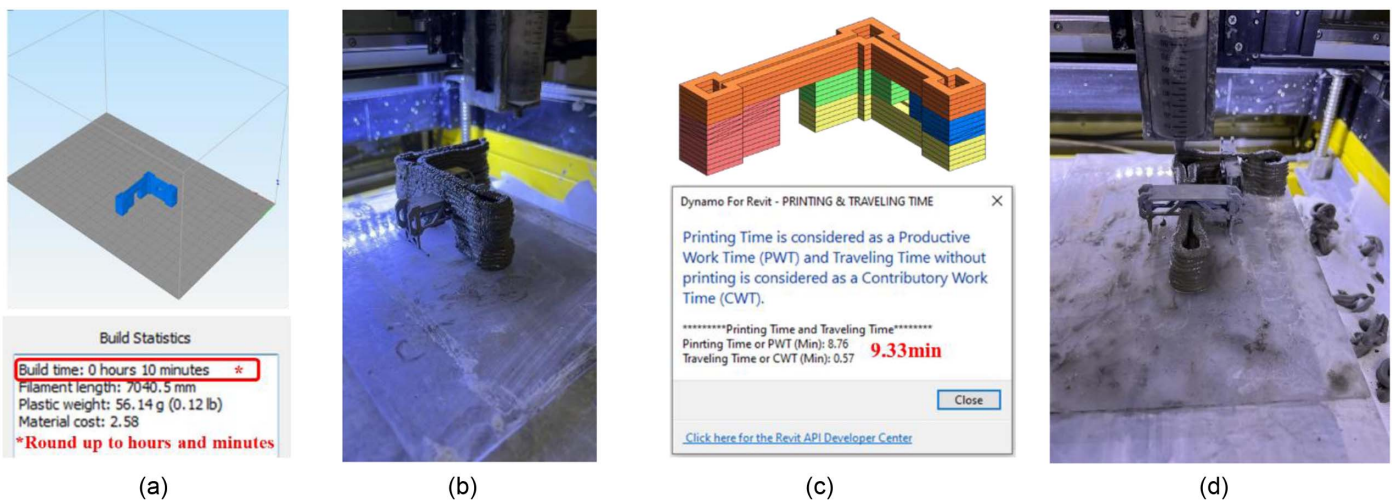


Fig. 17. Efficiency comparison between baseline slicers and proposed Dynamo: (a) printing time estimated using baseline slicer; (b) printed result for baseline slicer; (c) printing time estimated using the proposed Dynamo slicer; and (d) printed result for Dynamo slicer.

Table 2. Comparison among slicers based on estimated times for printing

Toolpath section	Baseline slicer			Dynamo slicer			Optimized slicer		
	T_{PW}	T_{CW+NCW}	T_{TOTAL}	T_{PW}	T_{CW+NCW}	T_{TOTAL}	T_{PW}	T_{CW+NCW}	T_{TOTAL}
Home-Start (min)	0.00	0.05	0.05	0.00	0.16	0.16	0.00	0.17	0.17
Start-End (min)	8.76	0.75	9.50	8.76	0.57	9.32	8.76	0.36	9.12
End-Home (min)	0.00	0.11	0.11	0.00	0.10	0.10	0.00	0.10	0.10
Total (min)	8.76	0.92	9.67	8.76	0.82	9.58	8.76	0.63	9.39
Δ Start-End (min)	—	—	—	0.00	0.18	0.18	0.00	0.38	0.38
Δ Start-End (%)	—	—	—	0	24	2	0	51	4

Note: Bold highlights the lines corresponding to printing route section (Start-End).

0%. The baseline slicer estimation shown in Fig. 17(a) is rounded up to hours and minutes and does not break down the time into printing and traveling time. In contrast, Fig. 17(c) shows the estimated time using the Dynamo slicer, and a detailed breakdown of the time is provided.

The printing strategy for the proposed Dynamo slicer was defined by the Work Sets, which enables the user to define the phasing sequence. Fig. 17(c) illustrates the sequence of the five work sets. This sequence was strategically defined to expedite printing by reducing printer time ($T_{CW} + T_{NCW}$). In contrast, the baseline slicer's printing sequence relies solely on a bottom to top sequence without any special strategy [Fig. 17(a)]. Consequently, for the baseline slicer the nozzle needs to make as many jumps as there are work zones within a layer, and it does not move to the next layer until all filaments (work zones) in the current layer are printed. This approach aims to eliminate the risk of collisions with existing printed parts. This criterion is ideal for small printers, where there is insufficient space for the nozzle to operate below the plane of previously printed layers. However, this is not necessarily a constraint to larger 3DCP projects if a thorough analysis of the printer's kinematics is conducted in advance.

Table 2 presents a comprehensive time classification for each slicer, encompassing movements from the home position to the starting printing point (Home-Start), the printing route (Start-End), and from the last printing point to the home position (End-Home). Movements to and from the home position might incorporate unavoidable delays attributed to header and footer G-Code settings, which were not factored into the ultimate comparison. Specifically, to evaluate the efficiency of multiple slicers, the actual time measurements during the printing process were compared in the Start-End rows for the tested slicers. The printing time (T_{PW}) denotes the duration the nozzle was in motion during printing.

The traveling time includes both the time related to contributory movements (T_{CW}) and noncontributory movements (T_{NCW}).

Table 2 compares the results of three slicers: a baseline slicer, the Dynamo slicer developed for this research, and an optimized version of the Dynamo slicer that minimizes all unnecessary movements (T_{NCW} equal zero). In addition to comparing the time of the Start-End toolpath—a choice that avoided distortions from the movements relative to the home position—the comparative analysis considered estimated times based on the generated G-Codes because it was possible to classify the time easily based on the type of movements within the code. The printing time classification was also automated using a Dynamo script for the time analysis and was verified by manually computing the times using a spreadsheet; the outcomes showed no variations. Furthermore, actual time, captured via the printer, was used to verify that the total printing time was consistent with the estimated time; however, because it was not possible to break down the time for each time classification within the printer-captured time, these data were not included in Table 2.

Using the G-Codes generated by the baseline, Dynamo, and optimized slicers, Fig. 18 depicts the 3D MATLAB version 2023b plot of the tool paths for each slicer. Also, the 3D printing times based on the work time classification were specified at the bottom of each scenario. It is important to mention that vertical jumps were short and had less impact on traveling time than horizontal jumps. Consequently, Fig. 18(a) has a longer travel time because it includes more horizontal jumps than the other alternatives. For all three scenarios, the printing path (PW) is the same, signifying the T_{PW} is also the same.

Table 2 summarizes how the Dynamo versus the optimized version of the slicer affected the selection of start and end points for each of the 3D-printed filaments. The Dynamo slicer reduced

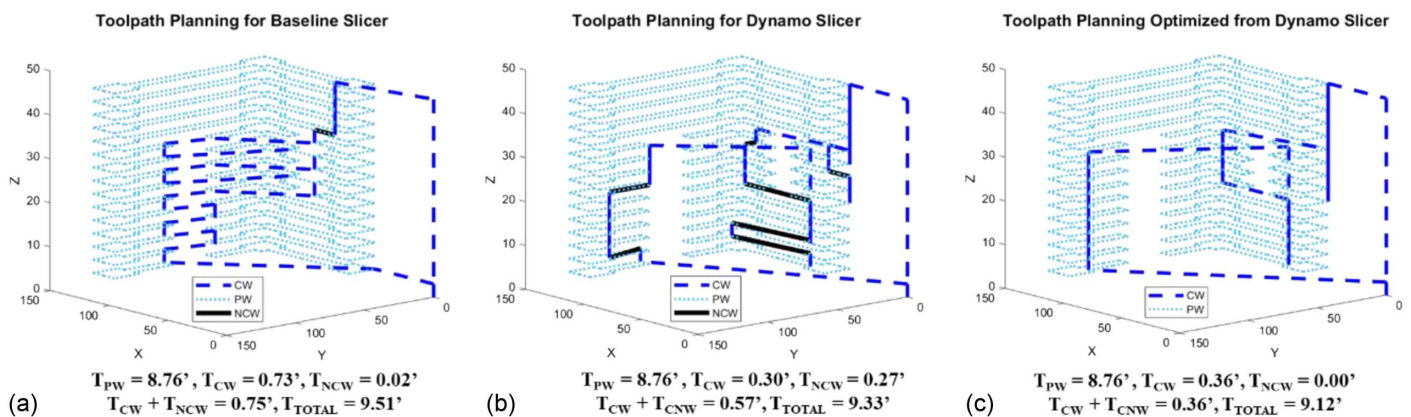


Fig. 18. Printing path of G-Codes generated with slicers' alternatives: (a) baseline slicer; (b) dynamo slicer; and (c) optimized slicer. The vertical z-axis scale has been magnified to improve toolpath visualization. PW CW, and NCW are shown.

the traveling time by 24% with respect to the baseline and reduced the total time by 2%. The optimized slicer, shown in Fig. 18(c), significantly reduced both traveling and total time by 51% and 4%, respectively. Although the total time could not be optimized significantly for these small-scale samples—which only take 10 min to print—the reduction in time could be substantial for larger-scale printers. These findings indicate that the proposed slicer can enable users to have a significant impact on the printing strategy. A customized printing sequence can reduce unnecessary traveling time for printers by implementing an alternative work phasing that avoids horizontal movements without printing.

Conclusion

Traditional 3D printing workflows suffer from fragmentation between the design and fabrication phases. Typically, a modeling tool exports only the geometry of the design into a slicer software program that generates the instructions for a 3D printer. In the case of construction, decision making is based on the use of a BIM model, which serves as the single data repository for project life cycle. Then, the BIM model should not lose the data from the design or the fabrication process.

Therefore, the main contribution of this paper consists of the development of a different approach compatible with the BIM methodology by enabling the integration of a single data repository for design, fabrication, and assembly. The proposed BIM methodology was implemented in Revit and Dynamo but can be exported to a nonproprietary IFC format, and the workflow could serve as a roadmap that can be replicated into other BIM authoring tools.

The proposed approach for automated modeling addressed all the gaps identified in the literature review (G_1 to G_7). For instance, the proposed workflow automates the modeling for the entire building system (G_1), considering construction details like wall openings for doors or windows (G_2) and 3D-printed formwork for columns (G_3). Also, the proposed BIM-Dynamo-slicer incorporates stop-start commands for the 3D printer (G_4) and incorporates all 3D-printed layers with their corresponding printing sequence that facilitates the understanding of the construction process (G_5). In addition, the proposed BIM workflow elevates the granularity of the model information up to a LOD 400 BIM model suitable for fabrication (G_6) and generates the G-Code for an entire building system, not just isolated geometries like previous studies (G_7).

Furthermore, several other contributions have been derived from the proposed approach. First, to the best of the authors' knowledge, this is the first work to implement a LOD 400 BIM model encompassing all the primary 3D-printed components of a 3DCP project. The complete modeling process was automated using a set of Dynamo scripts that eliminated the cumbersome process of manually modeling each of the 3D-printed layers. In addition, the proposed workflow automates the generation and population of BIM parameters to enrich the model.

Second, the resulting enriched model contains all the information generated during the slicing process that supplies users with a data repository for the planning process of the 3DCP project. Current workflows only extract the geometry related information from a LOD 200 BIM model and generate the printing sequence without the possibility to customize the printing strategy.

Third, the enriched LOD 400 BIM model has sufficient granularity for planning, coordination, and visualization. This higher granularity facilitates the phasing and work zoning process, which is not possible using previous workflows. The resulting enriched model can facilitate the spatial coordination with other building components because the geometry of all 3D-printed layers are

incorporated into the data repository. Because the model contains the printing sequence, all the information needed for the simulation of the printing process can be directly extracted from the BIM model. This process facilitates the visualization of the customized printing sequence, which is critical to guarantee a successful execution.

Fourth, using an enriched BIM model with planning parameters that define the project's printing sequence can help contractors customize the printing strategy. Previous work focused solely on the scenario of a continuous printing path, which is feasible only for isolated individual building components and not for a building system. Thus, the proposed workflow enables the definition of a user-customized G-Code that considers the construction phases based on the user's expertise. A summary video of the proposed workflow with Dynamo for Revit has been created by Rojas (2024).

Although the proposed workflow contributes to the body of knowledge, some limitations are worth noting. First, this paper focused on the dual nature of construction projects but did not delve into such tasks as robot kinematic simulation because these can be readily implemented using robotic programming plugins, e.g., Robots, and KUKAPrc (Allah et al. 2023). Second, this paper exclusively employed the sinusoidal infill pattern because it is the most found in 3DCP projects; however, it is worth noting that other infill patterns could be incorporated using similar Dynamo script workflows. Third, the cross section of the extruded 3D-printed filaments in the model was considered only for rectangular shapes defined by the extrusion width and layer height, which are prevalent in CC printers. Freely extruded filaments that have rounded profiles on both exposed faces of the 3D-printed filaments have not been integrated into the proposed tool.

Fourth, the assignment of work sets was not automated in the proposed workflow because these assignments depend on project requirements, printer limitations, and the construction strategy; however, manually assigning work sets to the printed filaments once these components are included in the BIM model is straightforward and efficient. Fifth, the proposed framework can be executed using Dynamo Player to eliminate the need for programming skills while still requiring basic familiarity with the Revit environment. Sixth, although the proposed framework has been tested for different types of columns (square, rectangular, and circular), and walls (straight, arcs, ellipse, circle, polygons), future studies are recommended to replicate the proposed framework for more complex shapes like nonplanar walls, or intricate surfaces. Lastly, the precision in defining the number of waypoints is based on the mesh generated in Dynamo. Enhanced smoothness can be achieved by employing nonuniform rational B-splines (NURBS) modeling or 3D splines for more complex shapes, particularly those with intricate surfaces.

Future research will involve analyzing alternatives, such as establishing a continuous path within a work set and restricting traveling time solely for transitioning to new work sets or incorporating collision avoidance features to create more robust and versatile solutions. Another important area to explore is the automation of work set phasing based on an optimization process that searches for the minimum traveling time but also analyzes the constraints related to the material (maximum number of printing layers due to material buildability), and the need for printing supports for overhangs and openings to validate the feasibility of printing options. Finally, future research can explore the potential of OpenBIM with an extension for the IFC4x3.2 standard to contemplate new 3DCP elements; the proposed attributes can be incorporated into a new schema of Property Sets (e.g., Pset_3DConcretePrintingElement-General) (buildingSMART 2024).

Data Availability Statement

Some or all data, models, or code that support the findings of this study are available from the corresponding author upon reasonable request.

Acknowledgments

This study was supported by the FW-HTF award from the National Science Foundation (No. 2128970). Any findings and recommendations in this material are those of the authors and do not necessarily reflect the views of NSF. The authors extend their sincere appreciation for the invaluable help and support received from Yu Wang, Dr. Pablo D. Zavattieri, Dr. Jan Olek, and Dr. Jeffrey P. Youngblood.

Author Contributions

Jorge Rojas: Conceptualization; Data curation; Formal analysis; Methodology; Visualization; Writing—original draft; Writing – review and editing. Sogand Hasanzadeh: Conceptualization; Data curation; Formal analysis; Funding acquisition; Methodology; Project administration; Resources; Software; Supervision; Writing – original draft; Writing – review and editing.

Notation

The following symbols are used in this paper:

- D_{ijk} = traveled distance;
- l_{ijk} = filament length;
- Sp_{ijk} = printing speed;
- St_{ijk} = traveling speed;
- T_{CW} = contributory work time;
- T_{NCW} = noncontributory work time; and
- T_{PW} = productive work time.

References

Abadia, P. P., S. Heine, K. Smarsly, P. Peralta Abadia, and H.-M. Ludwig. 2020. "A BIM-based approach towards additive manufacturing of concrete structures. Fault-tolerant sensor networks for wireless structural health monitoring view project." In *Proc., 27th Int. Workshop on Intelligent Computing in Engineering*. Berlin: Universitätsverlag der TU.

Abadia, P. P., and K. Smarsly. 2021. "An algorithmic BIM approach to advance concrete printing." In *Proc., 28th Int. Workshop on Intelligent Computing in Engineering*. Berlin: Universitätsverlag der TU.

Alabbasi, M., A. Agkathidis, and H. Chen. 2023. "Robotic 3D printing of concrete building components for residential buildings in Saudi Arabia." *Autom. Constr.* 148 (Apr): 104751. <https://doi.org/10.1016/j.autcon.2023.104751>.

Allah, T. B., W. Anane, and I. Iordanova. 2023. "Robotic additive manufacturing using a visual programming BIM environment." In *Proc., Canadian Society of Civil Engineering Annual Conf.*, 605–622. Cham, Switzerland: Springer.

Allouzi, R., W. Al-Azhari, and R. Allouzi. 2020. "Conventional construction and 3D printing: A comparison study on material cost in Jordan." *J. Eng.* 2020 (1): 1424682. <https://doi.org/10.1155/2020/1424682>.

BIMForum. 2023a. "Level of development (LOD) specification." Accessed May 12, 2024. <https://bimforum.org/resource/lo-d-level-of-development-1od-specification/>.

BIMForum. 2023b. "Level of development (LOD) specification (Part I)." Accessed May 12, 2024. <https://bimforum.org/wp-content/uploads/2023/10/LOD-Spec-2023-Part-I-2024-02-27.pdf>.

Böckin, D., and A. M. Tillman. 2019. "Environmental assessment of additive manufacturing in the automotive industry." *J. Cleaner Prod.* 226 (Mar): 977–987. <https://doi.org/10.1016/j.jclepro.2019.04.086>.

Bos, F. P., et al. 2022. "The realities of additively manufactured concrete structures in practice." *Cem. Concr. Res.* 156 (Jun): 106746. <https://doi.org/10.1016/j.cemconres.2022.106746>.

Boton, C., L. Rivest, O. Ghnaya, and M. Chouchen. 2021. "What is at the root of construction 4.0: A systematic review of the recent research effort." *Arch. Comput. Methods Eng.* 28 (4): 2331–2350. <https://doi.org/10.1007/s11831-020-09457-7>.

Breseghehlo, L., and R. Naboni. 2022. "Toolpath-based design for 3D concrete printing of carbon-efficient architectural structures." *Addit. Manuf.* 56 (Aug): 102872. <https://doi.org/10.1016/j.addma.2022.102872>.

Brioso, X., and C. Calderon-Hernandez. 2023. "Framework for integrating productive, contributory, and noncontributory work with safe and unsafe acts and conditions." *Int. J. Environ. Res. Public Health* 20 (4): 3412. <https://doi.org/10.3390/ijerph20043412>.

buildingSMART. 2024. "7.11 IfcStructuralElementsDomain—IFC 4.3.2 documentation." Accessed October 21, 2024. <https://ifc43-docs.standards.buildingsmart.org/IFC/RELEASE/IFC4x3/HTML/ifcstructuralelementsdomain/content.html>.

Buswell, R. A., W. R. Leal de Silva, S. Z. Jones, and J. Dirrenberger. 2018. "3D printing using concrete extrusion: A roadmap for research." *Cem. Concr. Res.* 112 (Oct): 37–49. <https://doi.org/10.1016/j.cemconres.2018.05.006>.

Correa, F. R. 2016. "Robot-oriented design for production in the context of building information modeling." In *Proc., 33rd ISARC*. New York: Curran Associates.

Davtalab, O., A. Kazemian, and B. Khoshnevis. 2018. "Perspectives on a BIM-integrated software platform for robotic construction through contour crafting." *Autom. Constr.* 89 (Sep): 13–23. <https://doi.org/10.1016/j.autcon.2018.01.006>.

Davtalab, O., A. Kazemian, X. Yuan, and B. Khoshnevis. 2022. "Automated inspection in robotic additive manufacturing using deep learning for layer deformation detection." *J. Intell. Manuf.* 33 (3): 771–784. <https://doi.org/10.1007/s10845-020-01684-w>.

Delgado Camacho, D., P. Clayton, W. J. O'Brien, C. Seepersad, M. Juenger, R. Ferron, and S. Salamone. 2018. "Applications of additive manufacturing in the construction industry—A forward-looking review." *Autom. Constr.* 89 (Mar): 110–119. <https://doi.org/10.1016/j.autcon.2017.12.031>.

Du, S., F. Teng, Z. Zhuang, D. Zhang, M. Li, H. Li, and Y. Weng. 2024. "A BIM-enabled robot control system for automated integration between rebar reinforcement and 3D concrete printing." *Virtual Phys. Prototyping* 19 (1): e2332423. <https://doi.org/10.1080/17452759.2024.2332423>.

El-Sayegh, S., L. Romdhane, and S. Manjikian. 2020. "Archives of civil and mechanical engineering." In *A critical review of 3D printing in construction: Benefits, challenges, and risks*. New York: Springer.

Forcael, E., J. Pérez, Á. Vásquez, R. García-Alvarado, F. Orozco, and J. Sepúlveda. 2021. "Development of communication protocols between BIM elements and 3D concrete printing." *Appl. Sci.* 11 (16): 7226. <https://doi.org/10.3390/app11167226>.

Guamán-Rivera, R., A. Martínez-Rocamora, R. García-Alvarado, C. Muñoz-Sanguinetti, L. F. González-Böhme, and F. Auat-Cheein. 2022. "Recent developments and challenges of 3D-printed construction: A review of research fronts." *Buildings* 12 (2): 229. <https://doi.org/10.3390/buildings12020229>.

Hao, B., and G. Lin. 2020. "3D printing technology and its application in industrial manufacturing." *IOP Conf. Ser.: Mater. Sci. Eng.* 782 (2): 022065. <https://doi.org/10.1088/1757-899X/782/2/022065>.

He, R., M. Li, V. J. L. Gan, and J. Ma. 2021. "BIM-enabled computerized design and digital fabrication of industrialized buildings: A case study." *J. Cleaner Prod.* 278 (Jan): 123505. <https://doi.org/10.1016/j.jclepro.2020.123505>.

Heidarnezhad, F., and Q. Zhang. 2022. "Shotcrete based 3D concrete printing: State of art, challenges, and opportunities." *Constr. Build. Mater.* 323 (Mar): 126545. <https://doi.org/10.1016/j.conbuildmat.2022.126545>.

- Hoffmann, M., S. Skibicki, P. Pankratow, A. Zieliński, M. Pajor, and M. Techman. 2020. "Automation in the construction of a 3D-printed concrete wall with the use of a lintel gripper." *Materials* 13 (8): 1800. <https://doi.org/10.3390/ma13081800>.
- Hossain, M. A., A. Zhumabekova, S. C. Paul, and J. R. Kim. 2020. "A review of 3D printing in construction and its impact on the labor market." *Sustainability* 12 (20): 8492. <https://doi.org/10.3390/su12208492>.
- Jabbari, A., I. D. Tommelein, and P. M. Kaminsky. 2020. "Workload leveling based on work space zoning for takt planning." *Autom. Constr.* 118 (Oct): 103223. <https://doi.org/10.1016/j.autcon.2020.103223>.
- Khamis, A. A., S. A. Ibrahim, M. A. Khateb, H. Abdel-Fatah, and M. A. Barakat. 2022. "Introducing the architecture parametric design procedure: From concept to execution." *IOP Conf. Ser.: Earth Environ. Sci.* 1056 (1): 012004. <https://doi.org/10.1088/1755-1315/1056/1/012004>.
- Kim, S., S. Chang, and D. Castro-Lacouture. 2020. "Dynamic modeling for analyzing impacts of skilled labor shortage on construction project management." *J. Manage. Eng.* 36 (1): 04019035. [https://doi.org/10.1061/\(ASCE\)ME.1943-5479.0000720](https://doi.org/10.1061/(ASCE)ME.1943-5479.0000720).
- Kreider, R. G., and J. I. Messner. 2013. *The uses of BIM classifying and selecting BIM uses*. University Park, PA: Pennsylvania State Univ.
- Lim, S., R. A. Buswell, T. T. Le, S. A. Austin, A. G. F. Gibb, and T. Thorpe. 2012. "Developments in construction-scale additive manufacturing processes." *Autom. Constr.* 21 (1): 262–268. <https://doi.org/10.1016/j.autcon.2011.06.010>.
- Lowke, D., E. Dini, A. Perrot, D. Weger, C. Gehlen, and B. Dillenburger. 2018. "Particle-bed 3D printing in concrete construction—Possibilities and challenges." *Cem. Concr. Res.* 112 (Mar): 50–65. <https://doi.org/10.1016/j.cemconres.2018.05.018>.
- Manogharan, G., R. A. Wysk, and O. L. A. Harrysson. 2016. "Additive manufacturing-integrated hybrid manufacturing and subtractive processes: Economic model and analysis." *Int. J. Comput. Integr. Manuf.* 29 (5): 473–488. <https://doi.org/10.1080/0951192X.2015.1067920>.
- Mechtcherine, V., V. N. Nerella, F. Will, M. Näther, J. Otto, and M. Krause. 2019. "Large-scale digital concrete construction—CONPrint3D concept for on-site, monolithic 3D-printing." *Autom. Constr.* 107 (Nov): 102933. <https://doi.org/10.1016/j.autcon.2019.102933>.
- Menegon, J., and L. C. P. da Silva Filho. 2022. "The impact of industry 4.0 concepts and technologies on different phases of construction project lifecycle: A literature review." *Iran. J. Sci. Technol. Trans. Civ. Eng.* 47 (3): 1293–1319. <https://doi.org/10.1007/s40996-022-00989-5>.
- Monteiro, H., G. Carmona-Aparicio, I. Lei, and M. Despeisse. 2022. "Energy and material efficiency strategies enabled by metal additive manufacturing—A review for the aeronautic and aerospace sectors." *Energy Rep.* 8 (Mar): 298–305. <https://doi.org/10.1016/j.egy.2022.01.035>.
- NIBS (National Institute of Building Sciences). 2020. *2020 Annual report to the president of the United States*. Washington, DC: NIBS.
- Pessoa, S., A. S. Guimarães, S. S. Lucas, and N. Simões. 2021. "3D printing in the construction industry—A systematic review of the thermal performance in buildings." *Renewable Sustainable Energy Rev.* 141 (May): 110794. <https://doi.org/10.1016/j.rser.2021.110794>.
- Rezvani Ghomi, E., F. Khosravi, R. E. Neisiany, S. Singh, and S. Ramakrishna. 2021. "Future of additive manufacturing in healthcare." *Curr. Opin. Biomed. Eng.* 17 (Mar): 100255. <https://doi.org/10.1016/j.cobme.2020.100255>.
- Rojas, J. 2024. "An integrated BIM planning workflow for 3D concrete printing projects." Accessed May 12, 2024. <https://youtu.be/Ts7lWFqzalw>.
- Roscoe, S., P. D. Cousins, and R. Handfield. 2023. "Transitioning additive manufacturing from rapid prototyping to high-volume production: A case study of complex final products." *J. Prod. Innovation Manage.* 40 (4): 554–576. <https://doi.org/10.1111/jpim.12673>.
- Sakin, M., and Y. C. Kiroglu. 2017. "3D printing of buildings: Construction of the sustainable houses of the future by BIM." *Energy Procedia* 134 (Oct): 702–711. <https://doi.org/10.1016/j.egypro.2017.09.562>.
- Siddika, A., M. A. Al Mamun, W. Ferdous, A. K. Saha, and R. Alyousef. 2020. "3D-printed concrete: Applications, performance, and challenges." *J. Sustainable Cem.-Based Mater.* 9 (3): 127–164. <https://doi.org/10.1080/21650373.2019.1705199>.
- Slepicka, M., S. Vilgertshofer, and A. Borrmann. 2021. "Fabrication information modeling: Closing the gap between building information modeling and digital fabrication." In *Proc., 38th ISARC*. Dubai, United Arab Emirates: International Association on Automation and Robotics in Construction. <https://doi.org/10.22260/ISARC2021/0004>.
- Smarsly, K., P. Peralta, D. Luckey, S. Heine, and H. M. Ludwig. 2021. "BIM-based concrete printing." In *Proc., 18th Int. Conf. on Computing in Civil and Building Engineering. ICCCBE 2020. Lecture Notes in Civil Engineering*, 992–1002. Cham, Switzerland: Springer.
- Stern, A., Y. Rosenthal, N. Dresler, and D. Ashkenazi. 2019. "Additive manufacturing: An education strategy for engineering students." *Addit. Manuf.* 27 (Mar): 503–514. <https://doi.org/10.1016/j.addma.2019.04.001>.
- Teng, F., M. Li, D. Zhang, H. Li, and Y. Weng. 2023. "BIM-enabled collaborative-robots 3D concrete printing to construct MiC with reinforcement." *HKIE Trans.* 30 (1): 106–115. <https://doi.org/10.33430/V30N1THIE-2022-0023>.
- Tu, H., Z. Wei, A. Bahrami, N. Ben Kahla, A. Ahmad, and Y. O. Özkılıç. 2023. "Recent advancements and future trends in 3D concrete printing using waste materials." *Dev. Built Environ.* 16 (Dec): 100187. <https://doi.org/10.1016/j.dibe.2023.100187>.
- Valtonen, I., S. Rautio, and J.-M. Lehtonen. 2023. "Designing resilient military logistics with additive manufacturing." *Continuity Resilience Rev.* 5 (1): 1–16. <https://doi.org/10.1108/CRR-08-2022-0015>.
- Weng, Y., N. A. N. Mohamed, B. J. S. Lee, N. J. H. Gan, M. Li, M. Jen Tan, H. Li, and S. Qian. 2021. "Extracting BIM information for lattice tool-path planning in digital concrete printing with developed dynamo script: A case study." *J. Comput. Civ. Eng.* 35 (3): 05021001. [https://doi.org/10.1061/\(ASCE\)CP.1943-5487.0000964](https://doi.org/10.1061/(ASCE)CP.1943-5487.0000964).
- Zikulnig, J., S. Chang, J. Bito, L. Rauter, A. Roshanghias, S. Carrara, and J. Kosel. 2023. "Printed electronics technologies for additive manufacturing of hybrid electronic sensor systems." *Adv. Sens. Res.* 2 (7): 2200073. <https://doi.org/10.1002/adrs.202200073>.